Optics & Laser Technology 146 (2022) 107554

Contents lists available at ScienceDirect

Optics and Laser Technology

journal homepage: www.elsevier.com/locate/optlastec

Laser-based hybrid micromachining processes: A review

Ashish Kumar Sahu, Jitin Malhotra, Sunil Jha *

Department of Mechanical Engineering, Indian Institute of Technology Delhi, 110016, India

ARTICLE INFO

Keywords:
Laser beam machining
Hybrid machining
Surface roughness
Sequential machining
LAECM
JECM
Vibration-assisted machining
Magnetic field-assisted machining
Electric field-assisted machining
Gas-assisted machining
Fluid-assisted machining
Drilling
Micromachining

ABSTRACT

Laser beam micromachining is a prominent method for micromachining applications. But it has some drawbacks like thermal stresses, uncontrolled dimensions, burrs, and spatter. Similarly, non-conventional processes like ECM, EDM, and conventional machining processes, namely turning, drilling and milling, also have limitations due to slow process and tooling costs. Researchers are continuously seeking hybrid machining, like laser-based hybrid machining methods, to improve the product's quality characteristics. Researchers have thoroughly investigated the laser-based hybrid process mechanism in the last decade and have identified different issues and control strategies to improve its performance. This paper reviews laser-based hybrid micromachining processes (LHMMP) in which LBM is combined with conventional processes and non-conventional processes in an assisted or sequential manner. Also, other energy sources assisting the laser beam machining process, viz. vibration, magnetic field, electric field, fluids, and gases, are reviewed in the current work. This paper summarizes the work performed on metals, non-metals and ceramics in the area of the LHMMP to create 3D micro features. Theoretical and experimental studies, mechanisms of machining, machining setups, and the impact of process parameters on laser-based hybrid micromachining techniques are reviewed in detail. The hybrid processes elevate the process efficiency, surface quality, tooling cost and precision of fabricated parts. In the last section of this paper, future development efforts needed in this area of laser-based hybrid machining are suggested to multiply the process utility.

1. Introduction

Micromanufacturing is becoming an eminent methodology having its feet in varied sectors like electronics, telecommunication, defence, automotive, aircraft, IT industries, home appliances, medical instruments, biomedical, implants industries, etc. [1–5]. Micro-products or micro-components usually have minimum requirements called micro-manufactured, ranging from a few μm to 1000 μm. Micro products can have complex 3D shapes with R_a values higher than 0.5 μm, high tolerances typically below 1 μm on a wide span of materials, including ceramics, steels, specialized alloys, etc. [6]. Traditional micro-manufacturing covers technological processes like machining, material deposition, forming, heat treatments, newly introduced additive manufacturing, and many more [7]. Significant applications are microreactors, microfluidic devices, micro moulds, micro dies, micro fuel cells [8–10].

Micromachining processes are still in the development phase and suffer from a lack of findings. Further research can push the processes from a lab centric environment to an industrial application scenario [11]. A list of critical challenges faced by researchers in micromachining is 3D geometries and complicated shape machining, satisfying requirements of surface finish, workpiece material limitations, high precision machining, machining time reduction, high production cost, etc. [12–14]. Now it's time to overcome these challenges in manufacturing high-quality products and fulfil industry demands [15].

The classification of micromachining processes is similar to macro machining processes and is divided into conventional, non-conventional, and hybrid micromachining methods, as shown in Fig. 1

Abbreviations: **LBM**, Laser Beam Machining; **LHMMP**, Laser-Based Hybrid Micromachining Process; **VALBM**, Vibration-Assisted LBM; **MFALBM**, Magnetic Field-Assisted LBM; **FALBM**, Fluid-Assisted LBM; **EFALBM**, Electric Field-Assisted LBM; **GALBM**, Gas-Assisted LBM; **LAM**, Laser-Assisted Milling; **LAECM**, Laser-Assisted ECM; **LAT**, Laser-Assisted Turning; **ECM**, Electro-Chemical Machining; **EDM**, Electrical Discharge Machining; **IT**, Information Technology; **FEA**, Finite Element Analysis; **LBT**, Laser Beam Turning; **LBC**, Laser Beam Cutting; **HAZ**, heat affected zone; **Fs**, femtosecond; **ns**, nanosecond; **MRR**, material removal rate; **SR**, surface roughness; **RP**, Rapid Prototyping; **MRF**, Magneto-Rheological Finishing; **ECH**, Electro-Chemical Honing; **CPS**, Cyber-Physical System; **IEG**, inter-electrode gap; **RCL**, recast layer; **MEMS**, Micro-Electro-Mechanical System; **LIPMM**, Laser-Induced Plasma Micromachining; **LAECM**, Laser-Assisted Electrochemical Machining.

* Corresponding author.
E-mail address: suniljha@mech.iitd.ac.in (S. Jha).

https://doi.org/10.1016/j.optlastec.2021.107554
Received 6 February 2021; Received in revised form 22 July 2021; Accepted 23 September 2021
Available online 30 September 2021

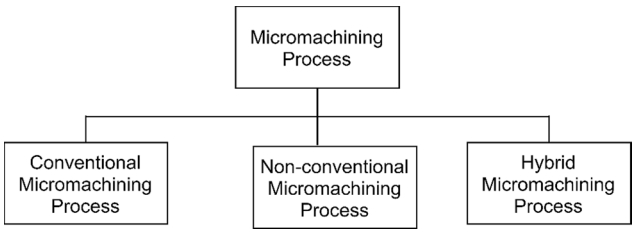

Fig. 1. Classification of the micromachining processes.

[16]. In the conventional micromachining process, an interaction between a tool and a workpiece results in a shearing action, and material removal happens. Although factors like cutting force and tool wear come into the picture due to the physical contact between tool & workpiece [17]. Conventional processes include micro-turning, micro-milling, & micro-grinding processes, where a single-point cutting tool or fine abrasive grinding wheel interacts with a workpiece material for material removal [18]. In the non-conventional process, no physical contact between the tool and work material happens. Machining occurs by energy transfer in other forms like sparks, vibration, electrolysis, beam energy (laser, electron, or ion), erosion energy [19–22]. In the hybrid process, two or more conventional or non-conventional processes are combined either in an assisted manner or in a sequential form so as energy sources of multiple processes can be used for machining [23,24]. The objective of using hybrid processes is to enhance the advantages or positives of one method and (or) reducing the disadvantages or negatives of the process to get the maximum benefit out of it.

Laser Beam Machining (LBM) is a well-established non-conventional micromachining process used for several industrial applications varying from one-dimensional to three-dimensional machining [25]. Laser beams are highly monochromatic, have high electromagnetic flux intensity with high spatial and temporal coherence. Laser beam properties make it highly directional and allow them to focus in narrow areas with increased intensity. The focused beam further enables them to deposit, remove or change the material properties by altering the inherent properties. Additionally, the laser's dynamic capabilities of depth and energy control make it more advantageous. A brief description of LBM is presented in the following subsection.

1.1. Laser beam Machining (LBM)

LBM is a thermal process that uses the focused beam energy for microfabrication applications. In this process, material ablation occurs by an intense laser beam radiation when the substrate absorbs the thermal energy. When the fluence generated by a focused beam is greater than the material threshold, it transforms the material into a molten, vaporized, and chemically degraded state. Ablation leads to material removal, resulting in the fabrication of geometry and surface modification at microns or sub-micron levels [29,170]. The sub-threshold value of laser fluence will result in permanent property modification of materials by forming HAZ. However, higher fluence leads to boiling of material and vapour bubble formation. The absorbed thermal energy is transferred to the surroundings by convection, as shown in Fig. 2.

When multiple pulses are used for laser ablation, the ablation thresholds may decrease due to the incubation effect. According to the Beer-Lambert law, the thickness or volume of material removed per pulse above the ablation threshold typically shows a logarithmic increase with fluence [26]. The thermal effect generated by laser beam depends on thermal & optical properties, surface characteristics, the microstructure of the material, and laser parameters. Thermal properties such as conductivity and specific heat; optical properties like reflectivity, absorption coefficient, density of a material, and refractive index majorly influence laser beam ablation characteristics [108]. Laser properties such as beam quality, pulse width, wavelength, and spot diameter also affect the interaction with the substrate. Thermal loss of laser fluence occurs due to reflectivity, conduction loss, and radiation losses from the substrate surface [27].

In LBM, material removal occurs due to fluence, so no cutting tool is required. This missing physical interaction behaviour leads to the absence of mechanically induced material damage, tool vibration, tool chatter, tool wear, and cutting forces. Nd: Yag and CO_2 are the most popular laser used for LBM applications. Nd: Yag laser gives high peak power in pulse mode. Fiber laser is also gaining popularity due to its robust nature and lesser maintenance. Shorter pulse widths such as ps and fs are preferred for high precision machining with lesser HAZ [28].

1.2. Laser beam machining variants

a) *Laser beam drilling* (**LBD**) is a precise non-contact technique that can form small diameter holes in a wide range of materials [30]. The upsides of laser drilling include the capacity to machine hard material, for example, superalloys, ceramics, and composites without any wear [31,32]. Laser micro-drilling having different techniques, namely single shot, percussion, helical, trepanning [33,34]. The

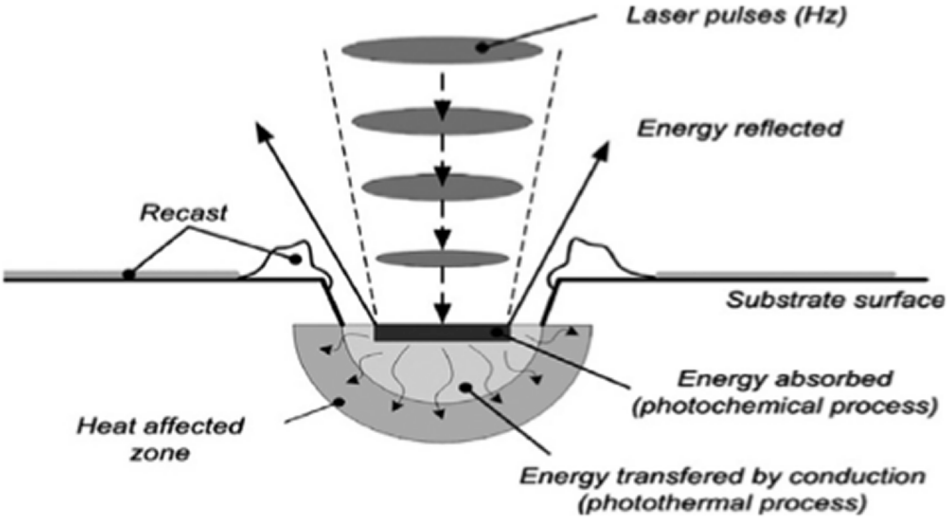

Fig. 2. Mechanism of the laser pulse and material interaction [29]. [Reproduced by permission of the publisher. Permission to reuse must be obtained from the rights holder].

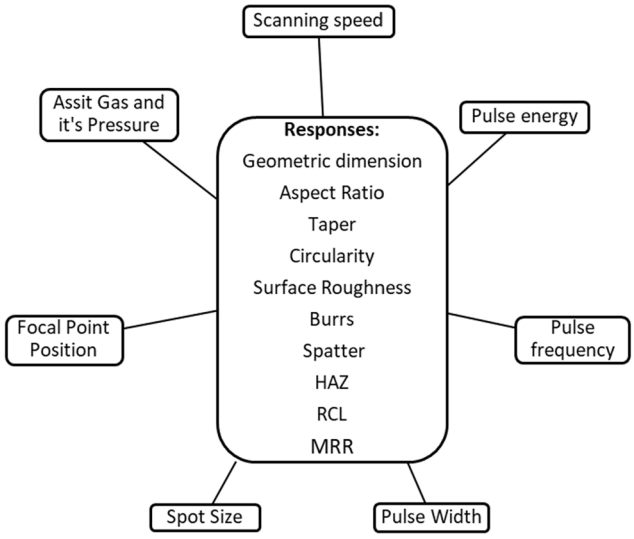

Fig. 3. LBM process parameters and responses.

drawbacks in LBD are the low aspect ratio while machining features (depth/diameter) and tapered hole profile because of focused beam shape condition.

b) *Laser beam turning* **(LBT)** is used to machine cylindrical-shaped or hollow cylindrical workpiece materials by removing micron level chips from the workpiece surface. Grooves on the cylindrical surface can also be created by this process [35]. Stent manufacturing on nitinol, stainless steel, and the biodegradable polymer is a potential application of laser beam turning in biomedical applications [36,37].

c) *Laser beam milling process* **(LBMP)** creates various geometries on metals and non-metals contrasted. LBMP has few interests points independent of material properties, such as hardness, thermal conductivity, and quick micro-scale component production [48]. The sub-variant of laser beam milling process, i.e., engraving and scribing, has applications for marking, cleaning, thin-film patterning, microchannels for fluid flow, and coining and moulding applications [38].

d) *Laser beam cutting* **(LBC)** is a widely used method of cutting sheets with laser fluence. The laser beam traverses along a cutting path with a defined scanning speed and melts the workpiece material. Nd: Yag or CO_2 laser cutting is used for different thicknesses depending on power and kerf width required. Excellent cut quality and narrow kerf width are the potentials of LBC [39,40].

e) *Laser beam polishing* **(LBP)** is a method to improve tribological properties and surface conditions, including microparts' waviness and roughness. Laser pulses of fs and ps range are utilized in this process, where melting of material in the range of 10–100 nm happens and results in a highly polished surface [154,155].

1.3. Challenges in LBM

Besides the advantages of LBM like faster machining, the small size of features, cost-effectiveness, and high production rate, few drawbacks exist. In laser drilling, lower aspect ratio, poor circularity, and taperness comes with burrs and spatter on hole inlet and outlet [34,52]. In laser milling, surface roughness, surface integrity, and microstructure change due to heat severely affecting the material properties. Machining reflective material like aluminium by LBM is still a challenge. Laser process parameters and response is shown in Fig. 3. Different researchers worked on the micro-drilling application to manufacture holes from few microns to 500 μm. They looked into problems associated with laser micro-drilling, i.e., hole taper, circularity and aspect ratio, etc. [53,54]. Few problems associated with LBM are mentioned below:

i. **Burr and spatter formation:** Spatter on the top and bottom surface of the workpiece is observed, which results in poor machining. Similarly, burrs on the bottom of the cutting surface are more in laser processing [55].
ii. **Surface roughness**: Surface roughness is poor in laser micromachining with larger pulse duration, i.e., ms and μs. In multiple scans, it increases drastically with larger pulses duration [56]. At a scanning speed lower speed surface, it is very rough due to the repositioning of melted material. Optimization of parameter needed for higher surface finish part.
iii. **Uncontrolled dimension of micro features**: Dimensional accuracy is a challenge in laser micromachining. The tolerance is weak and can't precisely shape features on the workpiece as the beam is tapered [49,57].
iv. **Recast layer and redeposition:** The machined zone's melted material gets redeposited, and the recast layer is constructed due to the unreachable region of assist gas or cooling effect [58]
v. **Thermal stress and crack**: The higher thermal intensity of laser beam and cooling effect of assist gases and thermal crack were observed on the machined surface. Due to thermal stress, a heat-affected zone (HAZ) is formed surroundings to the machined area [59].
vi. **Tapered surface**: Due to beam focusing condition, the tapered surfaces are achieved during machining in holes and channels [51,52,60].

1.4. Need of hybrid machining processes

The qualities like high precision, smaller dimensional tolerances, and superior surface structure are expected out of micro-components [57]. The application of micro-size components will be increasing extensively in the upcoming years. It is challenging to produce micro components with high productivity and less cost. LBM alone cannot give final products, which can be used for various applications because of drawbacks like uncontrolled dimension and tapered surface [61]. Still, there is a need for post-processing techniques like etching, chemical bath, or finishing.

Laser beam machining has been studied since 1960, and its industrial application of technology was started by CO_2 laser. In 1965, the first production laser cutting machine was used to drill holes in diamond dies. Since then, technology was put into production to continuously improve the way to cut titanium for aerospace and textiles applications. In the present scenario, the LBM technique is wildly accepted in several industries and research organizations. Development of fs and ps laser leads to the application of machining of micro features with lesser HAZ and better surface quality.

Many researchers took an interest in LBM in recent decades, and many studies were reported related to different variants of LBM. Although, most of the research focuses on the effect of process parameters. **Wu et al.** constructed a micro-hole array on PU synthetic leather to improve water vapour permeability with different laser beam wavelengths and observed the morphology of holes created. It revealed that photochemical and photothermal ablation occurs at a wavelength of 355 nm. At the same time, only photothermal ablation occurs at IR wavelength (1064 nm). Also, water vapour permeability was increased with a decrease in the wavelength [41]. **Lash et al.** performed laser drilling on 0.025 mm–0.127 mm thick foils of copper, titanium, and iron at atmospheric pressure in air and argon assistance [42]. They reported the number of pulses required to drill a hole and claimed a four-times reduction in drilling time on titanium in the presence of argon. In comparison, no machining was evident on the surface of the foil of aluminium in argon.

Biffi et al. performed percussion micro-drilling on Ti (0.5 mm thick) with pulsed fiber ns laser to examine the impact of machining parameters on the quality of machined through holes, like diameter, taperness, circularity, area of top spatter, and surface morphology[43]. Exit hole

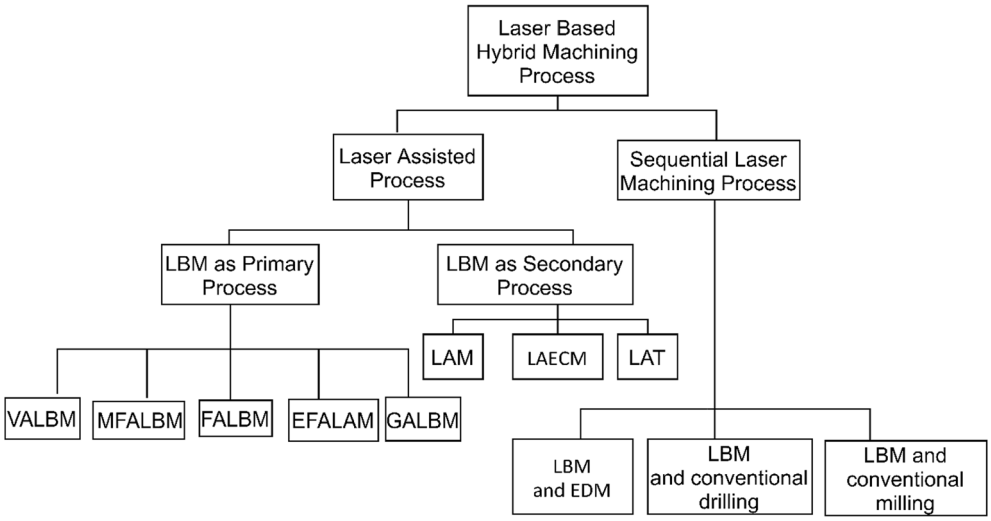

Fig. 4. Classification of laser-based hybrid micromachining processes. [**VALBM** Vibration assisted LBM; **MFALBM** Magnetic field-assisted LBM**; FALBM** Fluid assisted LBM; **EFALBM** Electric field-assisted LBM; **GALBM** Gas-assisted LBM; **LAM** Laser-assisted Milling; **LAECM** Laser-assisted ECM; **LAT** Laser-Assisted turning].

was free from spatter and dross, and also, D_{top} and D_{bottom} increased due to higher heat input. Taperness depends only on pulse energy, while pulse frequency doesn't make any contribution. The nano hardness of internal walls also resulted in a significantly higher value, which signifies the changes in Ti properties after the laser process on the hole's entrance and exit surface [44]. High aspect ratio drilling is still a challenge for LBM, and even a few studies like ref. [45,46] have reported these challenges. **Dhupal** et al. performed laser turning for manufacturing square micro-grooves on the cylindrical surface of ceramic materials. The effects of laser turning process parameters, i.e., lamp current, pulse repetition rate, pulse duration, scanning speed, and assist gas pressure on the quality of laser turned micro-grooves, were studied [35]. Similarly, **Kibria et al.** also employed laser machining to machine round bars of difficult-to-process ceramic materials with a single laser beam. The authors further studied the effect of process parameters on surface roughness and depth of cut in turning [47]. Other studies were reported in the laser micro-milling area to optimize geometrical dimensions and surface roughness of microchannel and different complex geometries [50,51].

The increasing number of publications per year on laser beam machining' state of the art establishment and process improvement reflects the academic attention towards the LBM process and can expect a more process-specific analysis in future. Several researchers have worked towards understanding the mechanism and processing condition for different materials with LBM. At present, the LBM process is in a phase where understanding the LBM process mechanism and productivity has to be enhanced by combining it with other hybrid machining processes. The hybrid machining processes based on laser also need to overcome the limitation of two or more processes to prove their usefulness.

The hybrid machining process, still being in the improvement stage, can be widely accepted in industries working on fabricating microfluidic devices, bio-medical, electronic devices, etc. The need for an hour is to transfer the available knowledge to the industries and newcomers in the field in a comprehensive way so that they can understand the process in a consolidated manner and think about possible ameliorations accordingly.

Other machining processes like EDM, ECM, or conventional machining also suffers from some drawbacks. EDM gives high-quality machining with high precision and better surface characteristics, but it is time-consuming, resulting in lesser production rates [62,63]. Also, it is limited to electrically conductive material [19,20]. ECM does not cause any thermal stress or HAZ, but precision is very limited in the process [10,20]. However, in the LBM process, accuracy is better compared to other processes. It will depend on beam delivery and the optical system. With conventional machining, significant tool wear and tool cost issues were reported [64]. It is also challenging to use conventional micromachining processes as microtools cost is approximately 40–50% of the total component cost. So, for cost-effective production, it is a need of an hour to use other processes in combination with conventional machining. Hybrid machining methods can be utilized to overcome the limitation of these individual processes [65].

In this paper, laser-based hybrid processes are discussed, past experimentation and theoretical studies are reviewed. The laser-assisted machining process is considered, such as LAECM, vibration-assisted LBM, magnetic or electric field-assisted LBM, fluid or gas-assisted LBM, and laser-assisted conventional machining. In laser-assisted conventional machining and laser-assisted ECM, the laser beam is the secondary process, which helps in melting or heating the workpiece. The primary process is used to remove material, resulting in improved overall efficiency. In vibration-assisted LBM, magnetic or electric field-assisted LBM, fluid or gas-assisted LBM, the laser beam is the primary process that gets benefitted by vibration, magnetic field, electric field, liquid, or gasses, respectively. In sequential machining processes like EDM or drilling are combined sequentially with the laser beam drilling process.

The hybrid machining processes have applications primarily focused on fabricating micron size components, like microholes, microchannels, and 3D geometry on difficult to cut material (ceramics, metal, non-metal, and superalloys) [16,24,72]. These processes have achieved burr and defect-free surfaces with good surface finish and lesser thermal stress [66]. A summary of machining setup is also covered in this review, which is used for sequential and assisted machining processes combined with LBM. In the last section, challenges faced by researchers are curated with a direction towards future works and areas of improvement like the development of precision machines with high dynamic stiffness and accuracy for LHMMP. Different machining setup causes repositioning errors in product, so, there is a need for a device to align two machining setups or develop such precision multi-process machining setups [67,71]. Apart from that, measurements also play a vital role during manufacturing, so for high precision micro components, it is a must to measure geometric dimensions on the machining setup itself [68]. In situ measurement of geometric dimension and surface finish for high-quality parts is a mandate [69]. Research should not be bounded till process advancement and development, but also it needs to develop a machining setup that can be used in the industry for assisted and

sequential machining on the same machining system [21,71].

To do so, a review of the published literature covering all aspects of laser-based hybrid machining along with their essential evaluation highlighting conceivable future contributions is the ideal way out. Indeed, any review article covering all the exploratory and analytical aspects of the laser-based hybrid machining process is as yet not published up to the best of our insight. The current work targets to fill this gap by providing a comprehensive and detailed review of laser-based hybrid machining processes focusing on the micromachining area.

2. Laser-based hybrid micromachining processes

Despite numerous research on micromachining techniques, it is still suffering from various limitations, as mentioned in the previous section. To overcome these limitations, researchers focused on hybrid machining techniques. In hybrid machining techniques, two or more machining processes are combined in an assisted or sequential way. Both processes have different machining principles, compound the advantages, and offset each other's limitations [65,163]. Hybrid manufacturing process performance and responses are better than individual machining processes. The laser-based hybrid process can be classified in an assisted and sequential manner, as depicted in Fig. 4.

There is one primary participating machining method in assisted machining methods, which is directly involved in material removal. At the same time, the secondary process provides assistance to increase metal removing mechanism or overcome defects like roughness, burrs, recast layer, thermal stress [16,58,70]. Secondary assistance processes can be ultrasonic vibration, external magnetic field or electric field, fluid, gasses, or heat [71]. The laser-assisted process can be further subclassified into laser machining as the primary method and other energy sources assisting laser machining. In another sub-classification, laser beam assisting another machining process like ECM or conventional machining. In these processes, LBM acting as the secondary process, as shown in Fig. 4.

In hybrid micromachining, clustering multiple processes in a single setup is not realized, so the process is performed in multiple steps with more than one setup. So, two or more processes perform machining at a similar machining zone one after another, as s process chain to overcome drawbacks in a sequential manner. From a machining perspective, there is no significant difference; however, the second process works on the machined surface of the machined process. Sequential machining is when two or more machining methods are implemented one after another on the same or different machining setups [71]. In a sequential process, one method has been performed after another to overcome the limitations of both individually [72]. One other benefit of the laser process combined with conventional machining is to use the thermal energy of laser machining for softening material and a significant reduction in cutting forces and torque [73].

In the past, few researchers have combined processes like conventional drilling and EDM, laser and conventional drilling, but most of them are on different machining setups. Laser machining with traditional machining tools like micro-drilling is performed on two separate machines, but the process suffers significantly from alignment errors [74]. However, in sequential machining, equipment, maintenance, and operation costs become higher due to two or more machining sources. In sequential machining processes, energy sources should interact in the same machining area, one after another, in sequence [71].

Hybrid machining operation improves surface integrity and productivity, lesser tool wear rate and efficient machining. If the hybrid machining is performed on the same machine, repositioning error will be eliminated, and precise parts can be manufactured with a lower tolerance value. There is a need to develop an integrated system for precise machining to benefit from the machining capabilities and advantages of sequential machining [75].

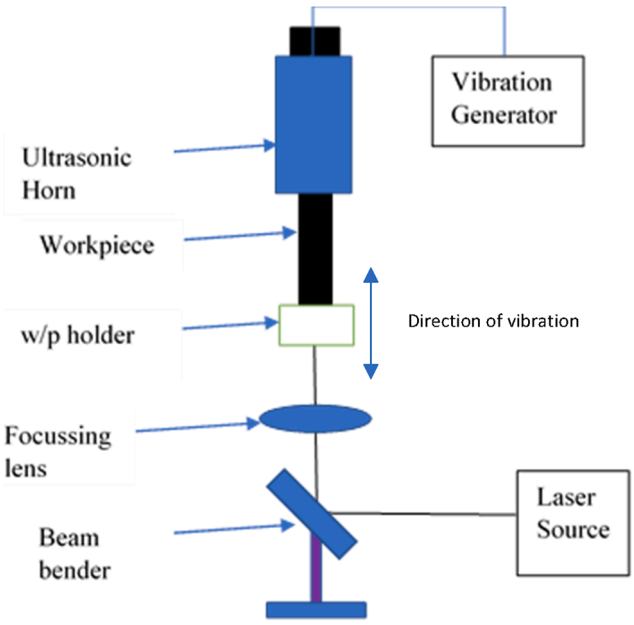

Fig. 5. US vibration LBM schematics [77].

3. Assisted machining with laser as primary process

In this section, studies about laser beam machining with external energy sources' assistance are described in detail. The energy in the form of vibration, external magnetic field, electric field, and fluids such as gasses and water helps laser micromachining improve fabricated parts quality and characteristics. Researchers have developed a lab setup for such processes and analyzed the mechanisms. Significant improvements are shown and concluded in the processes.

3.1. Vibration-assisted laser micromachining

The redeposited and re-solidified material layer is undesirable in laser machining, stopping interaction between the laser beam and fresh material and limiting aspect ratio and surface quality [76]. Reduction of re-deposition and post-processing of holes and channels is needed by chemical etching or polishing. Vibration-assisted EDM shows a better surface compared to typical EDM [171]. It needs to provide assistance to the workpiece or focusing lens by ultrasonic vibration and analyze the effect on redeposition and machining efficiency. Schematics are shown in Fig. 5 for the ultrasonic-assisted LBM process.

Zheng et al. proposed a novel method to fabricate high aspect ratio holes by vibration-assisted fs laser drilling system ($\lambda = 775$ nm) in which an ultrasonic horn is attached to the workpiece [77]. Ultrasonic vibration of frequency 40 kHz is installed on an adjustable post. The aspect ratio and surface finish of holes were improved with ultrasonic vibration on nitinol. Hole depth increased from 1.65 mm to 1.95 mm by using ultrasonic vibration assistance. Hole entrance diameter was increased and became irregular in shape in the presence of vibration. MRR improved significantly, and ultrasonic vibrations reduced the resolidified layer, so the surface appeared cleaner than without vibration assistance, as evident in 6(b). Vibration assistance also helps to lower down the redeposition of melted material as, shown in Fig. 6(a). The surface morphology gets improved with US assistance.

Laser hole drilling from the fine mask was carried out by **Choi et al.** on Invar alloy in which vibration changes the focal position of laser beam continuously [60]. The vibration was applied on the objective lens by a micro vibrator. Taper angle depends on the vibration and changes focal position. A regenerative amplifier-type fs laser based on Yb: KGW with a central wavelength of 1027 nm, average power of 6 W, was

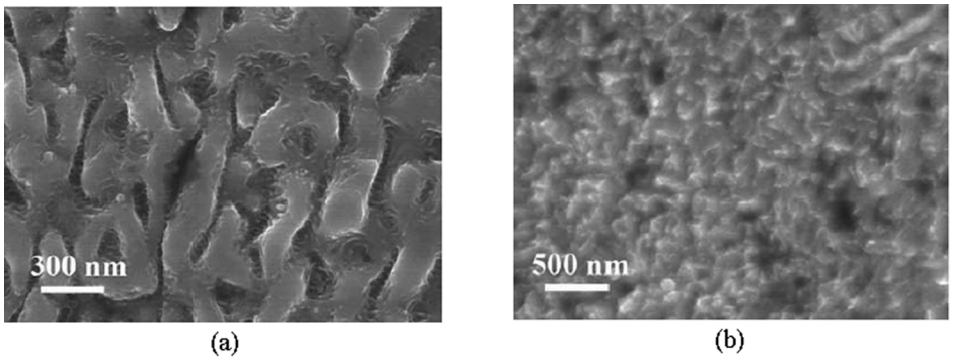

Fig. 6. (a) Material deposition without US assistance (*b*) with US-assistance [77]. [Reproduced by permission of the publisher. Permission to reuse must be obtained from the rights holder].

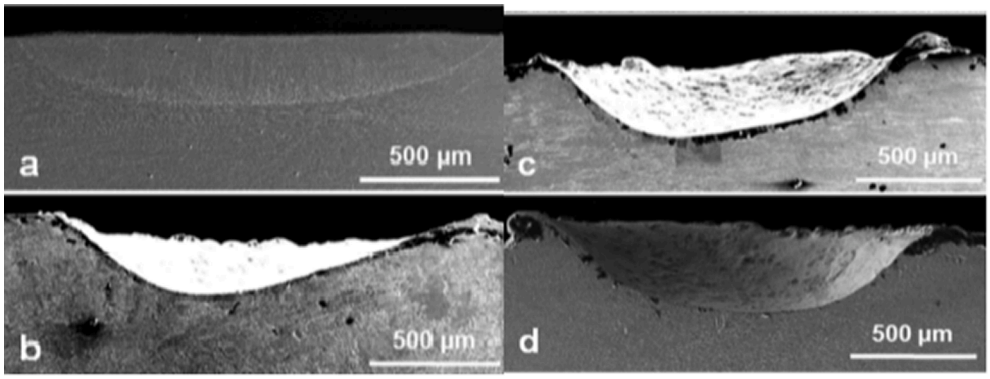

Fig. 7. SEM of cross surface irradiation at different ultrasonic power (a) 0% (b) 20% (c) 30% (d) 40% [78]. [Reproduced by permission of the publisher. Permission to reuse must be obtained from the rights holder].

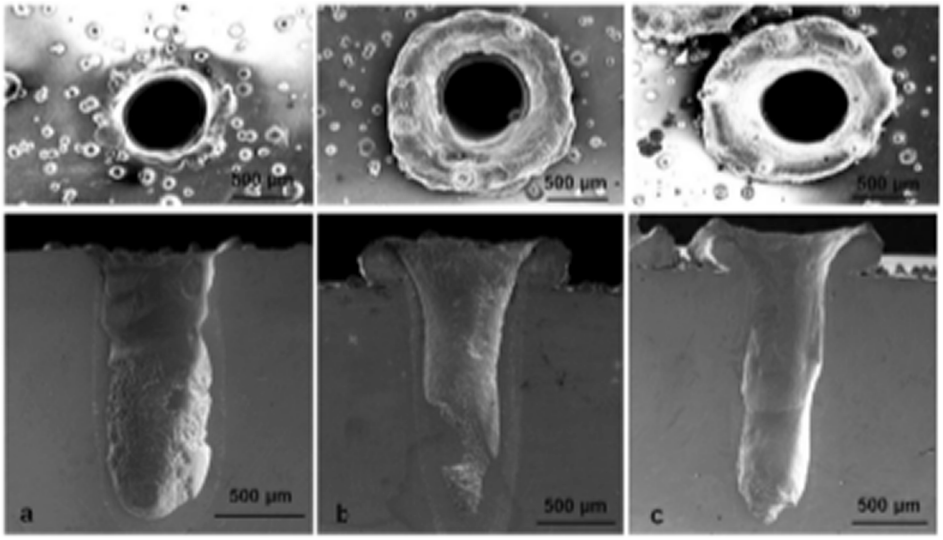

Fig. 8. Top surface and cross-section of a hole drilled (a) 20%, (b) 30%, (c) 40% of ultrasonic power [78]. [Reproduced by permission of the publisher. Permission to reuse must be obtained from the rights holder].

utilized in experiments. The workpiece's thickness was divided into five planes, and the laser pulse started striking on top plane position, and subsequent pulses focus moves downward plane and in a reverse manner. Eight pulses accumulated at one hole per vibration cycle. Five focal planes, including the sample front and back sides, were defined by dividing the material into four parts along its thickness. Focusing condition on top found the better result and was used for further analysis. The exit diameter changes rapidly compared to the entrance diameter with vibration amplitudes, which is evident by the taper angle. The hole taper depends on the amplitude of vibration, which varied between 31.8° and 43.9° at different amplitudes ranging from 1 to 13 μm at the frequency of 100 Hz. Taper angle was decreased with an increase in amplitude.

Melting and surface vaporization mechanism in argon and ultrasonic

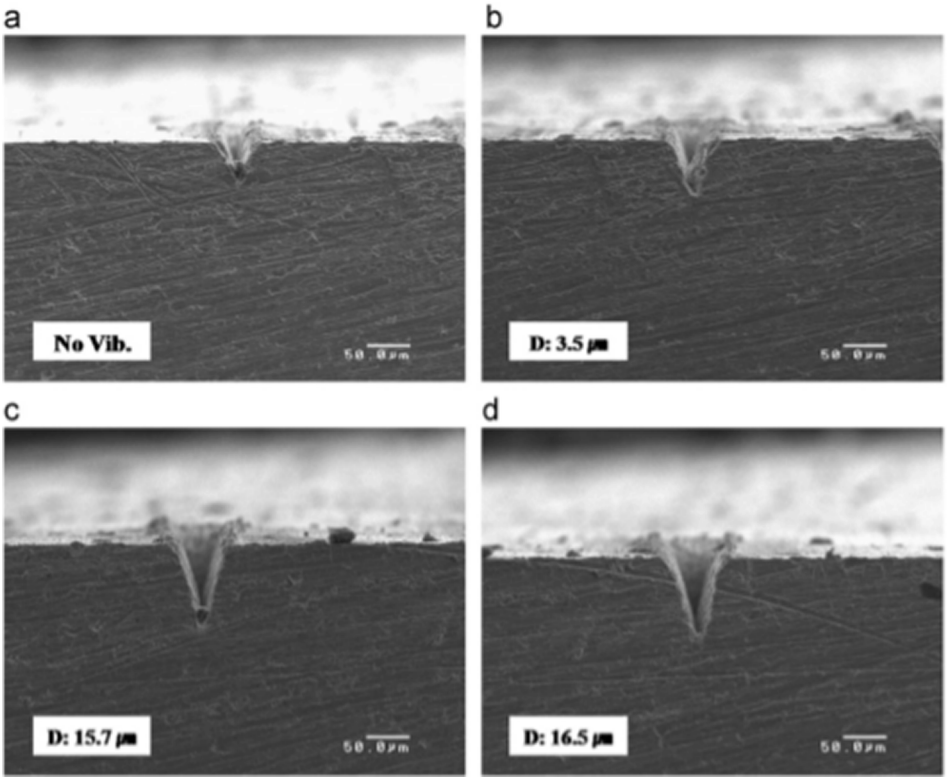

Fig. 9. Vibration displacement effect at 50 μJ/pulse energy with 500 Hz frequency of laser [79]. [Reproduced by permission of the publisher. Permission to reuse must be obtained from the rights holder].

vibration-assisted laser drilling understood by **Alavi et al**. on Stainless steel. Vibration of different amplitude range is given to the workpiece by continuous-wave CO_2 laser. It was observed that without vibration, a re-solidified region is visible on the workpiece surface. Increasing the amplitude of vibration increases the depth of the resolidified region with an increased diameter, as shown in Fig. 7 (a-d) [78]. Resolidified region is narrower without vibration, as seen in Fig. 7(a); However, applying vibration of different amplitude with similar laser irradiation results in material ablation and results in the deeper crater, as shown in Fig. 7 (b-d) can be seen. SEM image of cross-section shows that vibration assistance fabricates straight holes, and spatter is observed less at a lower amplitude of vibration. However, increasing vibration amplitude increases the redeposition of material surrounding holes, as shown in Fig. 8 (a-c). At lower ultrasonic power(20%), spatter can be seen surrounding to hole without any material built up. By increasing, ultrasonic power, heavy material built up clearly can be seen surrounding to hole. It appears in the early stage of melting, expulsion in the form of droplets.

Park et al. performed fs laser machining by applying ultrasonic vibrations to the focusing lens instead of the workpiece with pulse energy of 50 mJ/pulse and a scanning speed of 0.01 mm/s. The experimentation was performed by Ti sapphire fs laser at 795 nm wavelength. However, depth shows improvement with an increase in displacement heights, as exhibited in Fig. 9 [79]. With the introduction of vibration, heat transfer was more efficient due to local force convection. As a result, the ablated particles cooled faster and had less tendency to agglomerate.

Ultrasonic vibration assistance to LBM improves the surface quality. Redeposition and recast problems can also be solved by vibration assistance. Kang et al. applied ultrasonic vibration to the laser polishing method [164]. VALBM can create higher aspect ratio holes, and channels and upcoming research needs a wide range of experimentation and modelling of process on different metals and ceramics.

3.2. *Magnetic field-assisted LBM*

To improve LBM, researchers are looking into an opportunity in the

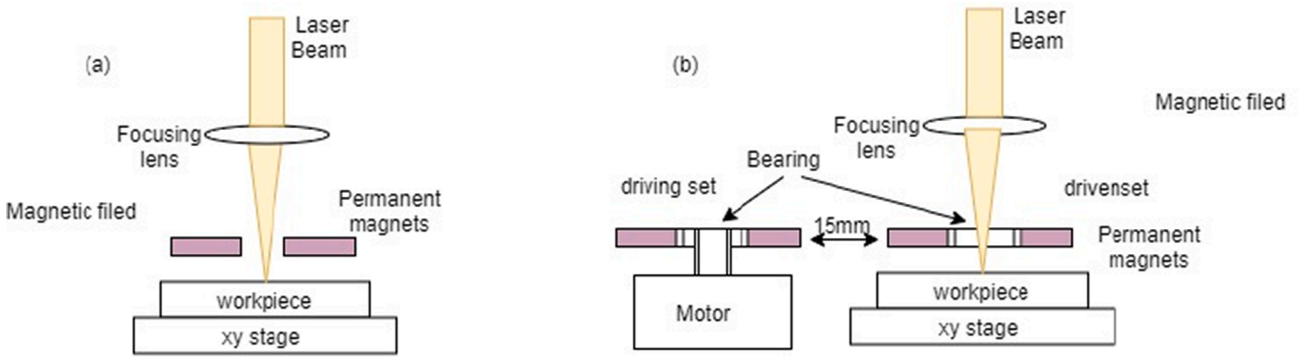

Fig. 10. (a) Static MFALMM (b) Dynamic MFALMM.

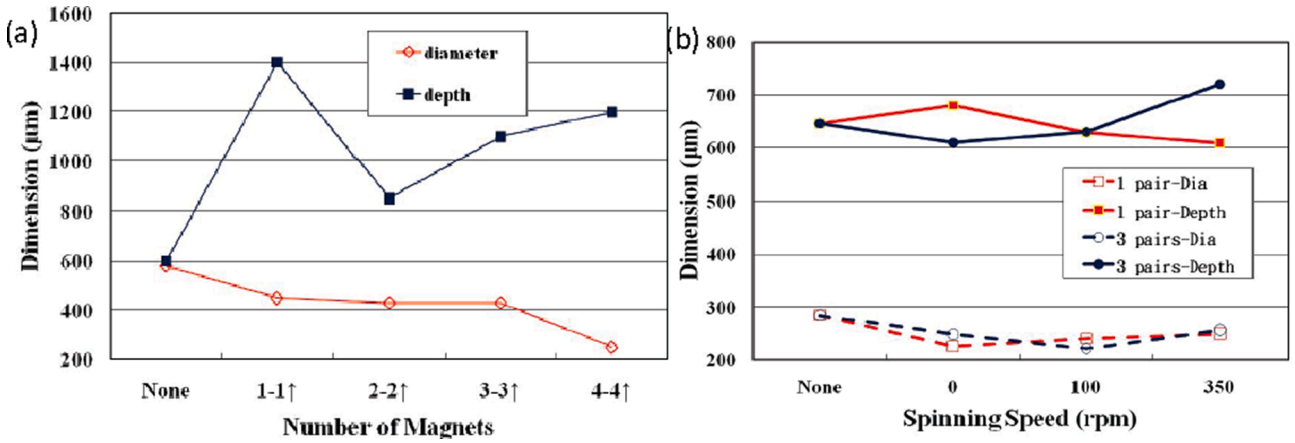

Fig. 11. Schematics of (a) Depth and (b) inlet diameter variation of holes with different magnets set and spinning speeds [53]. [Reproduced by permission of the publisher. Permission to reuse must be obtained from the rights holder].

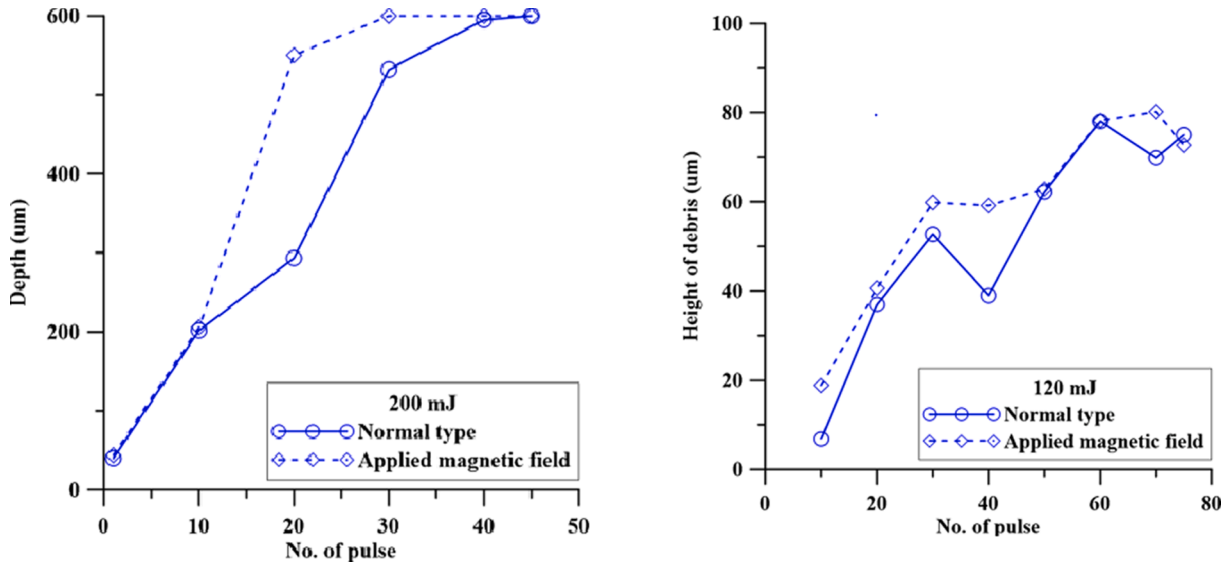

Fig. 12. Effect of magnetic field on debris diameter and height [80]. [Reproduced by permission of the publisher. Permission to reuse must be obtained from the rights holder].

area of magnetic field-assisted laser machining (MFALBM). An external magnetic field was created by permanent magnets and was applied to improve LBM process efficiency. The external magnetic field creates Lorentz force, which increases electron speed, boosts plasma density, and improves process performance [53,80]. MFALBM was tried on refective material, but it is still challenging for laser beam machining.

Machining of highly reflective Aluminum 6061 material (Reflectivity 90%) was performed with the MFALBM process with Nd: Yag laser at 532 nm (270 mJ pulse energy). Permanent magnets have developed static and dynamic magnetic fields, as shown in Fig. 10. For a static magnetic field, a permanent magnet was attached directly to the sample on both sides of the plate [53]. Drilling was performed at the interface of two plates. The dynamic magnetic field was developed by a hollow brass tube-driven set of permanent magnets attached to ball bearing, through which laser beam passes. The height of plasma was investigated at different magnetic fields. At the smaller magnetic field, the plasma was shorter. In the static magnetic field, the drilled hole profile was examined with different pairs of magnets and found depth is higher with the assisted magnetic field. The deepest hole was found with one pair of the magnet. The hole depth was increased by 133%, and the inlet diameter decreased by 33% in the magnetic field presence. In the dynamic magnetic field, depth and diameter were analyzed at different spinning speeds of 0,100 and 350 rpm. HAZ and inlet diameter was diminished by 37% and 30%, respectively. The diameter and depth did not affect spinning speed because of the non-uniform distribution of the magnetic field, resulting in magnets' rotation [53]. Depth and inlet diameter variation of holes with different magnets set and spinning speeds is shown in Fig. 11.

Ho et al. performed magnetic field-assisted laser percussion drilling to explore the feasibility of machining of highly reflective material Al5052 by ns Nd: Yag Laser (532 nm) [80]. A circular, hollow NdFeB permanent magnet of 10 mm diameter was used with a variable inner hole size of 1.5, 3, and 4.5 mm. The magnetic field's effect on the diameter of the hole, depth, height, and debris diameter was analyzed at a different pulse energy of 120 and 200 mJ. The quality of the hole was improved significantly in the magnetic field-assisted laser percussion drilling method. Depth of the hole had shown improvement by 87.7% without a magnetic field. This effect happened due to Lorentz force, which assists molten material in lifting upwards, and expansion of plasma increased the removal rate of material from the sidewall, as shown in Fig. 12(a). Similarly, debris height is shown improvement in the presence of a magnetic field (Fig. 12(b)).

An external unidirectional magnetic field was applied in laser-induced plasma micromachining (LIPMM) to improve the plasma

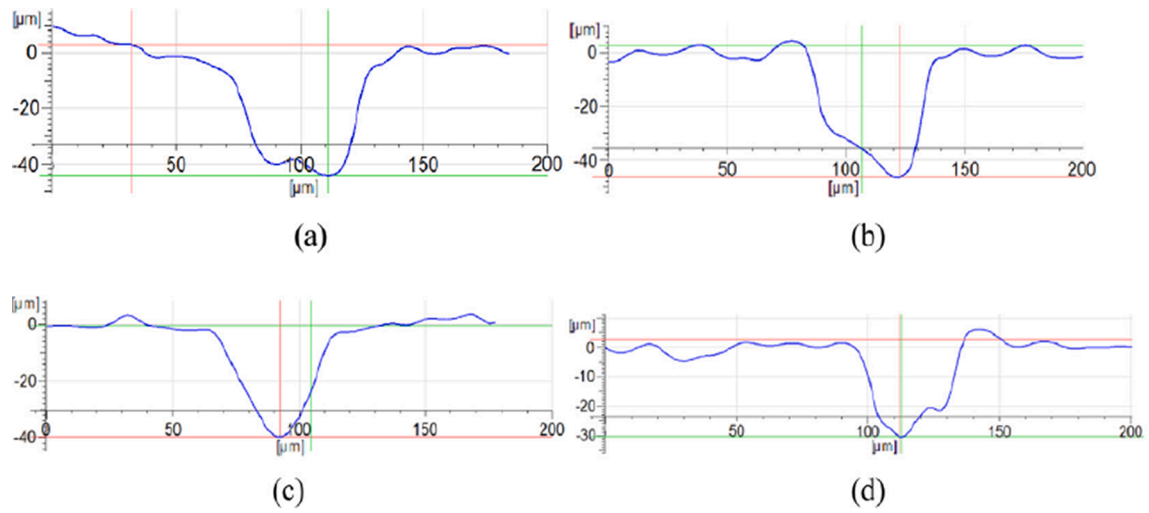

Fig. 13. Typical micro-channel cross-sections made by LIPMM in the presence of magnetic fields in configurations (a) longitudinal upward (b) downward (c) transverse (strength 5400 gauss) (d) without magnetic field [81]. [Reproduced by permission of the publisher. Permission to reuse must be obtained from the rights holder].

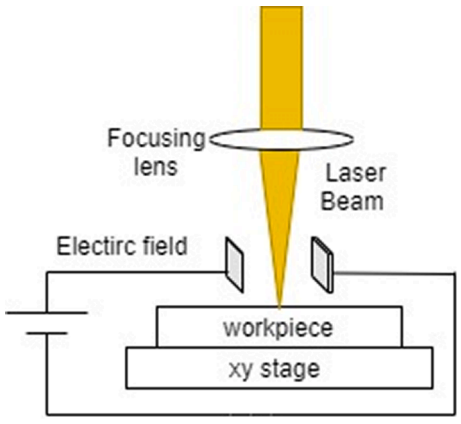

Fig. 14. Schematics of EFALBM [82].

characteristics of steel. Magnetic fields of different configurations of magnetic line direction were tried, namely longitudinal upward and downward, transverse to channel cross-section as shown in Fig. 13(a-d). Longitudinal fields lead to a more significant enhancement in plasma energy than transverse fields by the wider and deeper cavity. The channel's depth and width were increased with the magnetic field, which further improved the MRR [81].

The combined effect of the magnetic field, water and LBC was investigated by Wang et al. [165]. Magnetic field-assisted laser hole-cutting of magnesium alloys was explored systematically with and without using water immersion by fs and ms laser for blind holes and through holes. And, it was found that the magnetic field increases the entrance diameters for blind and through holes while decreases the blind-hole depth. The average grain size number in HAZ near the hole was improved for grain refinement by increasing the magnetic field strength [165].

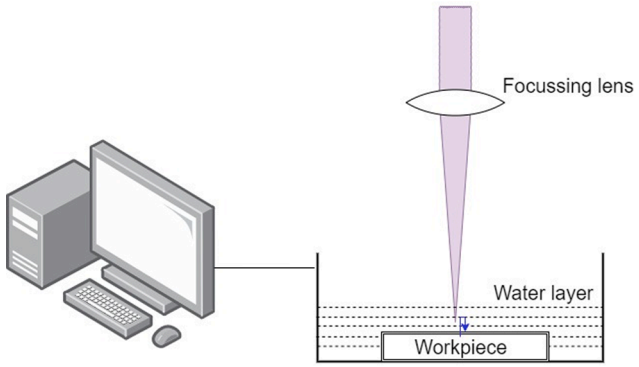

Fig. 15. Schematic diagram of underwater LBMM process [85].

3.3. *Electric field-assisted LBM*

Researchers also explored the possibility of electric field-assisted laser machining. Laser interaction phenomena were studied with the electric field. An external electric field was created with positive and negative terminal surroundings to the laser and material interaction zone, as shown in Fig. 14.

Chao et al. performed electric field-assisted laser percussion drilling for highly reflective material aluminium 5052 by ns Nd: Yag (532 nm). The effect of electric field and influence of different electrode configurations have been measured in penetration depth and inlet diameter [82]. Finite element analysis was conducted using Comsol software to simulate the electric field. Depth of penetration increases in the electric field medium because of the drilled material movement, which was accelerated by the external electric field applied by the electrode and electric force removed the charged particle.

Zheng et al. performed ultrashort laser pulse machining of silicon wafer for MEMS application. Electric field significantly affects the cleanliness of the surface and reduction of contamination [83]. Detailed data will be required to conclude the pro and cons of the EFALBM on a wide variety of materials.

Electric field assisted LBM still need to explore, and a significant contribution is needed in this area. Combinedly, ElectroMagnetic Field-Assisted Laser Process possibility also exploring by a few research groups [166]. In this decade, a newer methodology will be showing an impact on research.

3.4. *Fluid assisted-laser micromachining*

Laser micromachining assisted by fluids such as water, gases, alcohols, and the salty solution is described. Fluids-assisted laser micromachining solves drawbacks such as burrs, dross, re-deposition, and re-casting. However, fluids such as water also decrease thermal stresses and microcracks of surfaces [84]. Researchers have developed experimental

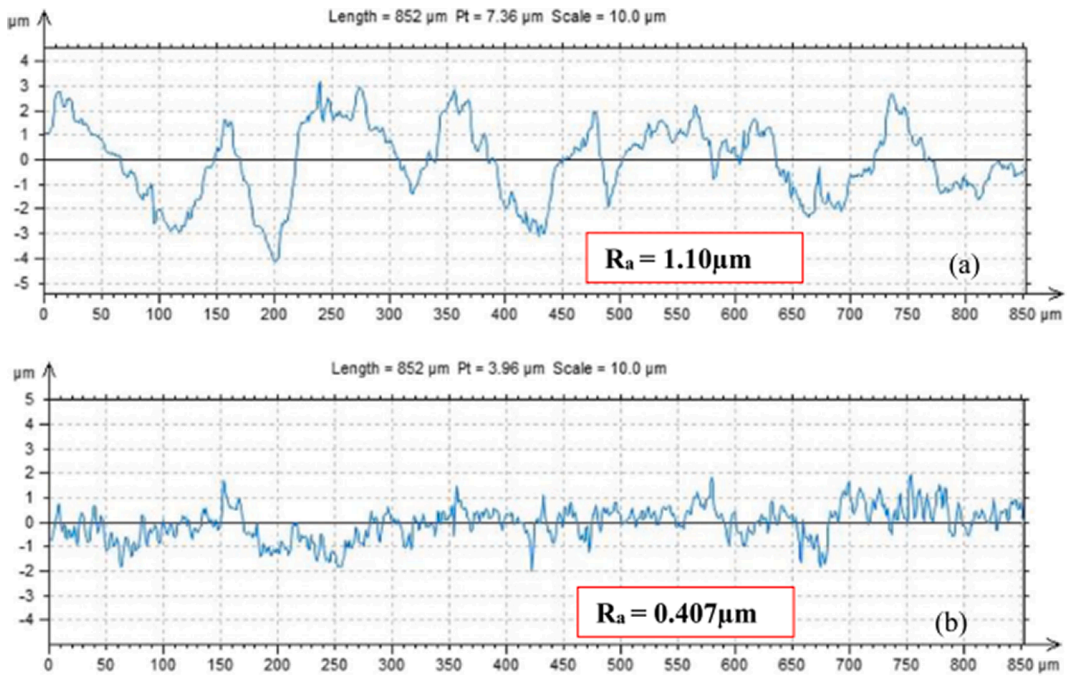

Fig. 16. Comparison of surface roughness of the microchannel in (a) air and (b) water [88]. [Reproduced by permission of the publisher. Permission to reuse must be obtained from the rights holder].

setups to analyze the process parameters' effect and understand material removal mechanism in these hybrid processes.

3.4.1. Water-assisted laser micromachining

Micro components like holes and channels were examined post-laser micromachining, and thermal drawbacks on surface quality were observed. The common thermal drawbacks observed are HAZ, recast layer, debris, and cracks. Thermal effects were present due to longer pulse width, such as millisecond to the microsecond, but the machining system with short pulse width like femtosecond and picosecond pulses are costlier. So, the water-assisted laser micromachining technique is utilized to diminish excessive heat in work material from the machining zone during ablation [85]. Along with machining, it was expected to heat work material from the machining zone amid removal. Fig. 15 shows a schematic of water-assisted LBM.

Recently few researchers proposed liquid-assisted LBM to overcome problems for different materials in different liquid mediums. The most popular liquid used is water, which is available at a low cost.

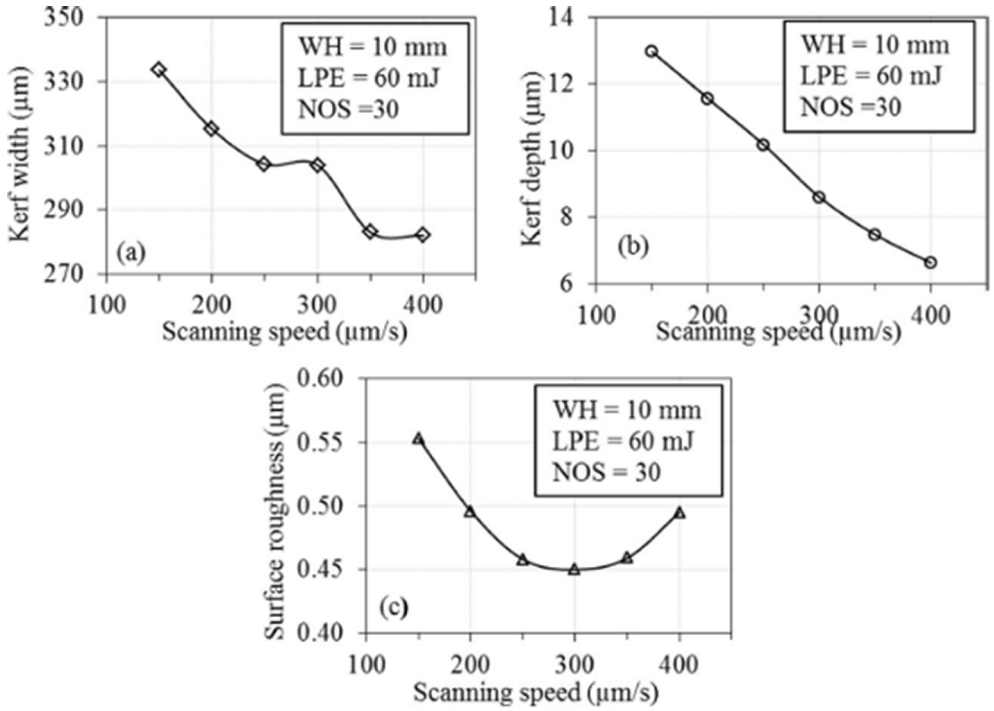

Fig. 17. Effect of scanning speed on (a) kerf width, (b) kerf depth (c) surface roughness, (WH = 10 mm) [88]. [Reproduced by permission of the publisher. Permission to reuse must be obtained from the rights holder].

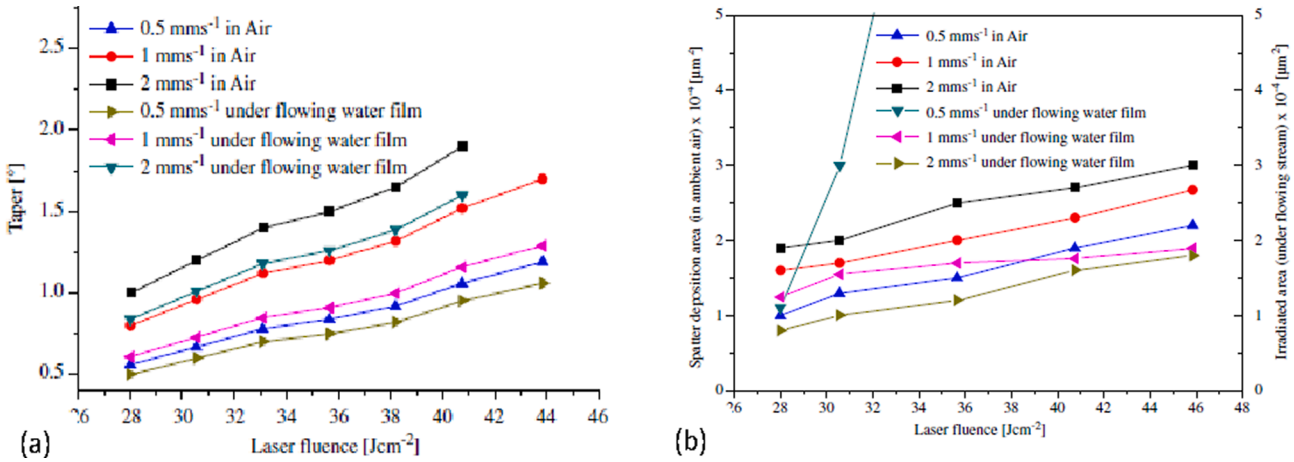

Fig. 18. (a) Effect of laser fluence on hole taper (b) spatter deposition and irritated areas for different scan speeds [90]. [Reproduced by permission of the publisher. Permission to reuse must be obtained from the rights holder].

Underwater or jet water-assisted LBM with different lasers like CO_2 and Nd: Yag was recently performed in a liquid-assisted machining format to minimize thermal stresses [86]. A thin layer of water covers the workpiece to remove excess heat and debris. If the layer is thick, then a significant loss of laser pulse energy was observed. The researchers also tried water-assisted machining by flowing water layer or water through the nozzle or as some droplet, but flowing water or by nozzle helped to improve MRR by removing debris from the machined zone and remove taperness of holes. **Mistry et al**. simulated liquid-assisted LBM by FEA technique [87].

Behera et al. implemented underwater Nd: Yag LBM and analyzed the thermal effect of the LBM process such as recast layer, HAZ, debris, and thermal crack for fabricating microchannels on stainless steel 304 [88]. They used a 10 mm thick water layer above the workpiece surface, maintained during machining. Surface roughness was observed 2.7 times lesser in water compared to air, as seen in Fig. 16. Elemental characterization concluded that oxygen percentage at the middle of the channel is higher in the air than underwater because of oxidized debris and recast layer ejected away by water. The cooling effect of water causes lesser oxidation of melted material. Optimum scanning speed, number of scans, and pulse energy obtained for better surface quality are shown in Fig. 17(a-c). In underwater LBM, kerf width and depth showed the same trend as dry LBM, in which both dimensions decreases with scanning speed. However, roughness decreases first then start increasing with scanning speed, as shown in Fig. 17(a-c)

Underwater laser ablation was carried out by **Wuttisarn et al.** to improve the metal removal and reduce thermal damage [89]. A nanosecond pulse laser with a wavelength of 1064 nm, pulse duration of 120 ns, and pulse frequency of 30 kHz was used in this study. Water was supplied by a nozzle of 3 mm diameter at an angle of 45° at lower pressure to improve metal removal. Experiments were performed by ns pulse laser of 1064 nm wavelength with 70% scan overlap and spot size

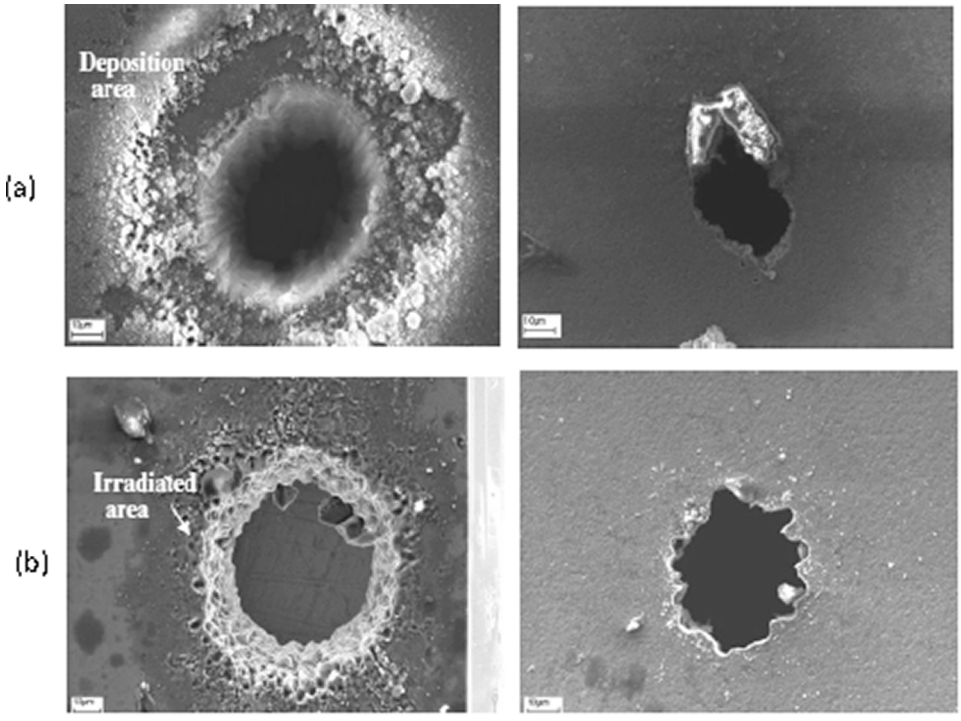

Fig. 19. Entrance and exit hole diameter in (a) air and (b) water.[90]. [Reproduced by permission of the publisher. Permission to reuse must be obtained from the rights holder].

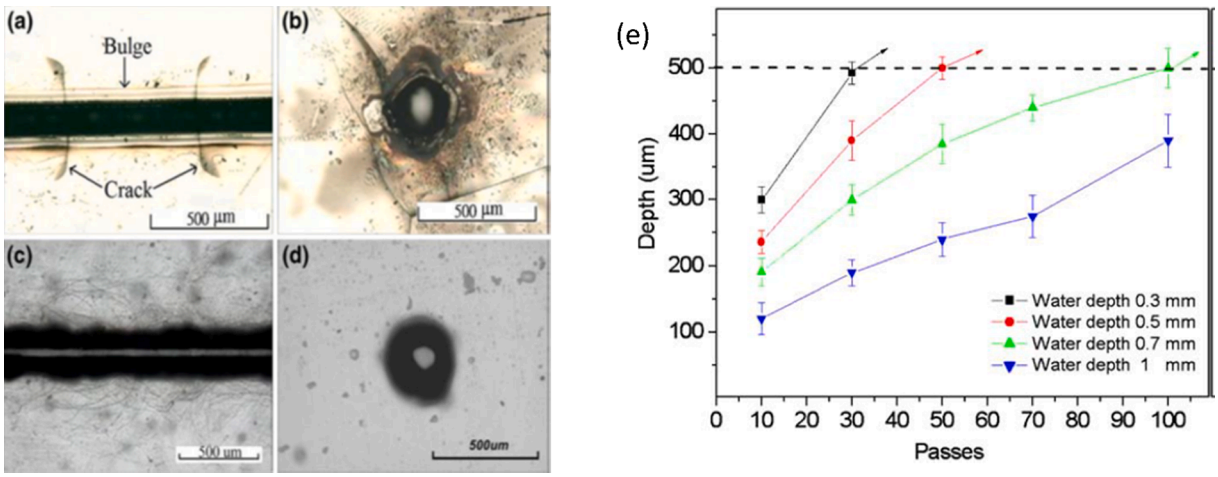

Fig. 20. Comparison of a linear channel in (a) air (c) underwater; hole in (b) air (d) water (e) effect of water depth on the etching depth [91]. [Reproduced by permission of the publisher. Permission to reuse must be obtained from the rights holder].

of 20.3 μm on titanium alloy (Ti6Al4V) sheet. Surface morphology was compared in air, underwater layer, and flowing water, which showed flowing water film achieved higher depth than the stationary water layer. The laser travel speed effect was also analyzed on cavity depth and taper angle with different water flow rates. A higher flow rate increases the depth and reduces taperness. This higher flow rate was caused by the momentum of water, which can induce a more significant amount of material removal and stepper cut profile with a lower taper.

Micro-drilling of 50 μm of hole size on silicon sheets is performed in the air and underwater stream using the trepanning technique. A water layer of 1 mm above the workpiece is available during laser drilling [90]. **Wee et al.** studied the impacts of laser parameters on scattering deposition, irradiated area, and taper. Lower scanning speed is suitable for minimum hole taperness, spatter deposition, and irradiated areas underwater compared to the air shown in Fig. 18(a,b). The poor circularity of the hole at the exit in air drilling and a small exit area was observed. This is because of material solidification at the entrance. The less irradiated area was observed in underwater machining because of less redeposition of material, and residual inside holes were cleaned by water as exhibited by Fig. 19(a, b).

Crack less fluidic channels and holes were fabricated underwater by laser micromachining on pyrex glass by **Chung et** al. [91]. CO_2 laser equipment performed the laser ablation with a maximum laser power of 30 W. The thermal cracks were absent in underwater machining. This was primarily attributed due to the occurrence of crack failure due to thermal stress, so through cutting had difficulty, as shown in Fig. 20 (a-d). A smaller water depth is required through cutting with fewer passes, as evident in Fig. 20(e). Lower water depth for the higher thickness may cause cracks due to insufficient cooling.

High-speed fabrication of microchamber for microfluidic application was carried out by **An et al.** Water assisted fs laser drilling was performed on silica glass in this study [92]. Inner walls of microfluidic chambers were analyzed by SEM and were found improvement in surface roughness due to water ablation. There was a too-short time for material interaction and inadequate ablation at high scanning speeds, whereas bubbles prevent water from removing debris efficiently at slow speeds. The single and double microchamber microfluidic devices were successfully fabricated.

In another study, **An et al.** fabricated a nozzle (i.e., through-hole) on microfluidic devices to sort out the problem of nozzle alignment during assembly over microchannel by water-assisted fs laser machining on glass [93]. A bubble was formed in a water droplet, which removed debris from the machining zone. After machining, a gap of 2 s was maintained to allow water droplets to carry debris with them. This method was found effective to fabricate complicated microfluidic systems.

Laser machining followed by water quenching of alumina was analyzed by **Barnes et al.** [94] using continuous-wave CO_2 laser with an x–y computer numerical controlled (CNC) positioning. First, a layer of 1–2 mm of water was spread on the w/p surface, which was removed by constant air stream flow and making the laser spot dry, as shown in the schematic diagram Fig. 21. A comparison of water-assisted with dry laser machining was carried out. A temperature profile was achieved using a thermocouple in HAZ to analyze thermal stresses during cutting. FEA was performed to predict temperature and stress is HAZ. Analysis of cracks on different power and feed rates in both conditions, i.e., the laser alone and water-assisted, was shown in Fig. 22 (a, b).

Water assisted fs laser helical drilling was compared with the air medium of alumina ceramic [167]. Water assistance increased the hole entry and exit diameters, reduced the taper angle, and increased the hole cross-section area. Water assistance could reduce the amounts of residual debris and redeposition of ablated material on the hole sidewall. There was almost no residual debris and redeposition of ablated material on the hole sidewall near the hole exit.

The researcher tried to combined gas and water-assisted laser machining in few studies available [168,169]. Spray mist assisted laser

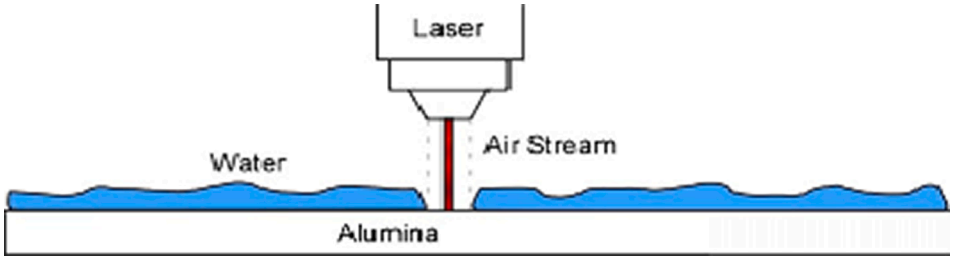

Fig. 21. Schematic of laser and air stream with water layer [94].

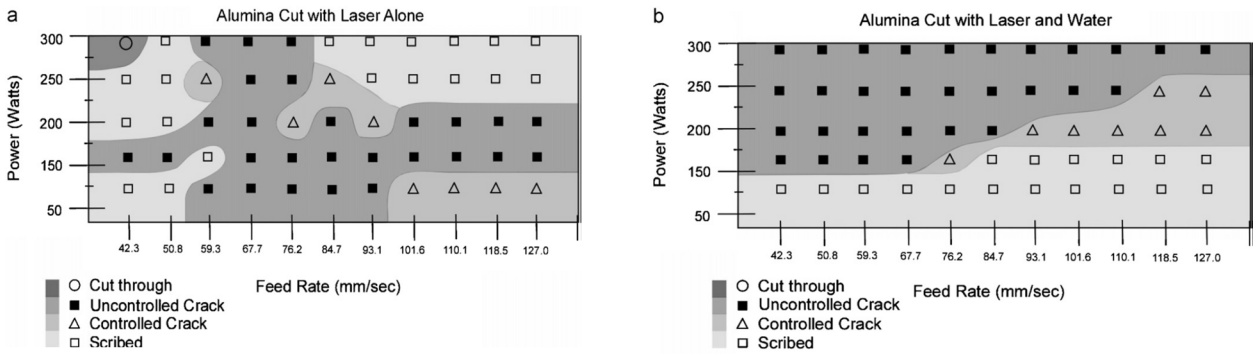

Fig. 22. Process maps based on power and feed rate (a) Alumina cut with laser (b) Alumina cut with laser and water [94]. [Reproduced by permission of the publisher. Permission to reuse must be obtained from the rights holder].

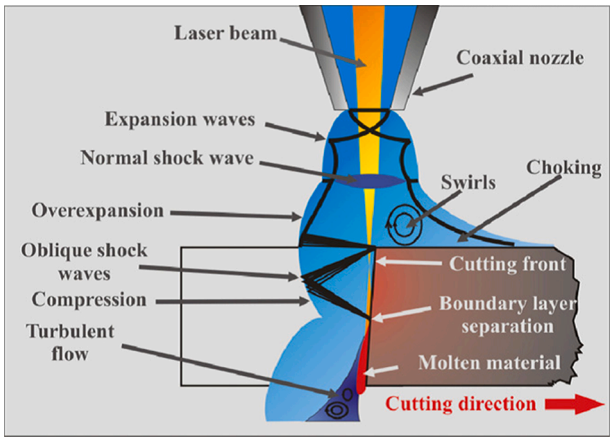

Fig. 23. Aerodynamic interactions in LBC using a conical sonic nozzle [153]. [Reproduced by permission of the publisher. Permission to reuse must be obtained from the rights holder].

machining technology forms a thin and fast-flowing water film on the CVD diamond coating surfaces [168]. Sprayed droplets were radially dispersed from the impingement point and an ellipse-shaped water film zone due to the nozzle's tilt. Spray assisted method was found better compared to underwater and dry machining.

Water assisted LBM reduces thermal stress and cracks on the workpiece surface. It reduces HAZ around the drilled hole or channel. Also, significant improvements in surface roughness is observed in this process.

3.4.2. *Gas-assisted LBM*

Assist gas aids in cutting and evacuates molten material from the kerf. It plays a crucial role in laser fusion [95,96]. The molten material is removed out due to aerodynamic interaction between molten metal and assists gases, which has an enormous effect on cutting quality and produces flow separation phenomena, as shown in Fig. 23 [95,153]. Another function of assist gas is to protect focusing optics against vapours or spatters from the interaction zone. Assist gas can be supplied coaxially in cutting head through nozzles. The problems associated with cutting quality can be solved by controlling assist gases pressure, which is controllable by a flow meter and depends on nozzle orifice diameter. Different gasses, i.e., argon, oxygen, nitrogen, air, helium, can be supplied during the process. When reactive gas such as oxygen is used, it delivers additional exothermic energy by chemically reacting with molten metal. This reaction supplies additional energy, which enhances the cutting process [97]. Inert gases such as argon, helium can be used for better cut quality and act as shielding [98].

Oxygen assisted laser cutting of mild steel is performed to analyze the oxidation reaction of iron [99]. An exothermic reaction took place, which produced a melted iron oxide layer (FeO) and was removed by oxygen pressure. A brittle layer of FeO of few microns was observed during cutting in the machining zone and was amorphous. The temperature of the melting zone had not reached the boiling temperature of FeO. Authors have further given guidelines to mild machine steel in oxygen assisted manner. High-speed cutting will be preferable in mild steel. The focused laser beam was passed through the nozzle co-axially with the oxygen jet. Nitrogen was also used sometimes in cutting, which does not react chemically in the melting zone.

Jurag et al. created 25 different structures on Austenite Cr-Ni steel (X5CrNi18-10) (1 mm thick sheet) with Nd: Yag laser considering process parameters like laser power, spot diameter, the position of a focal point in three different mediums, i.e., argon, air, ethyl alcohol. These structures were observed by confocal microscopy [100]. Oxidation of the surface took place in the air, which resulted in black coloured structures on the surface of the sample. In alcohol, no oxidation was

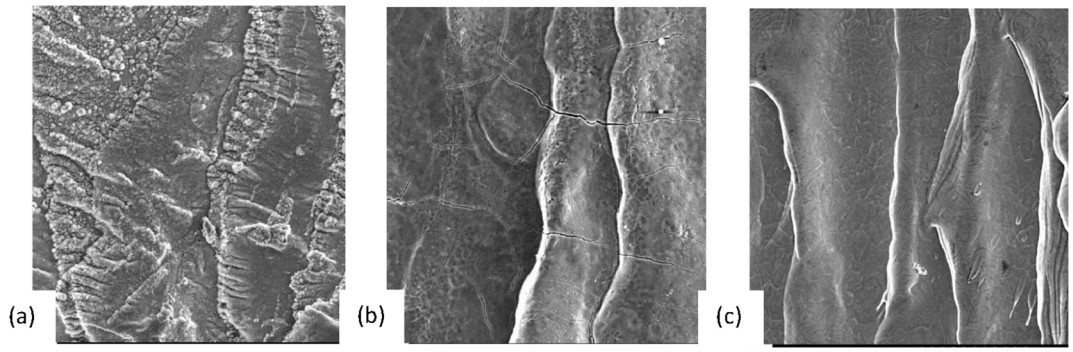

Fig. 24. Laser cut surface in different mediums (a) Nitrogen, (b) Compressed Air, (c) Argon [102]. [Reproduced by permission of the publisher. Permission to reuse must be obtained from the rights holder].

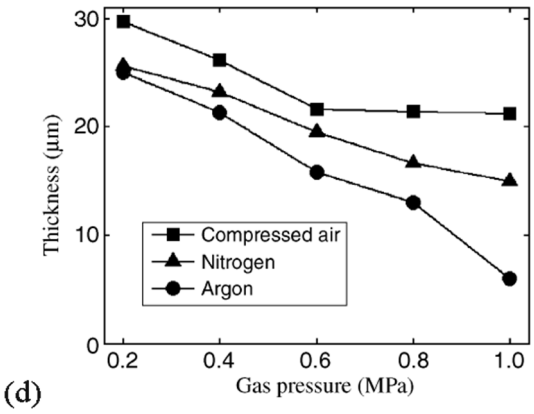

Fig. 25. HAZ layer thickness variation with gas pressure [102]. [Reproduced by permission of the publisher. Permission to reuse must be obtained from the rights holder].

observed, but laser character changed in specific areas of the structure. Other maximum and minimum MRR was studied in alcohol and air.

Micromachining of electrical grade silicon steel was performed to show the effects of shielding gas (He, Air, Ar, O_2) and gas pressure by **Jackson et al**. [101]. They used three lasers of 1064 nm, 532 nm, and 355 nm wavelengths, with a maximum power of 8,5 and 3 W. They found oxygen allows faster machinability of Si steel. However, the depth-etch rate was highly dependent on assist gas pressure. The melting of the surface was more prominent because of the fondness for oxygen. Silicon reacted with oxygen and produced a surface layer on the cut front of silicon dioxide (SiO_2). This formed a semi-impermeable seal over the underlying material, thereby inhibiting the reaction between the oxygen and the molten material. Machining in the presence of helium and argon leads to an oxide-free edge formation when examined with XRD. SEM image showed a considerable recast layer of high hardness that was difficult to remove.

LMM in three different gas, i.e., compressed air, argon, and nitrogen, was performed. Their effects on laser cut quality factor, HAZ, surface morphology and corrosion resistance of Titanium alloy were analyzed by **Shanjin et al.** [102]. Burning of the surface was observed, which produced wider kerf due to the exoergic reaction of oxygen. In the air medium, oxygen and nitrogen are present, which formed a thin layer of hard and brittle oxide and nitride reacting to Ti alloy, which resulted in wider HAZ. Microcracks were observed while cutting in the presence of oxygen, as shown in Fig. 24. These are due to the surface's tension force and the brittleness of titanium oxide and titanium nitride. Very small microcracks were also found when machining with nitrogen. The thickness of HAZ was more at a lower pressure due to the gas flow and cooling effect. The thickness of HAZ was lower in argon compared to others, as shown in Fig. 25. **Riveiro et al.** performed CO_2 laser cutting of Al-Cu alloy by coaxial supersonic nozzle for better cut quality and better MRR in assist gas medium [103].

In another study, laser cutting of aluminium in different mediums of assist gas Ar, N_2, O_2, and compressed air was performed [104]. The chemical composition of the surface of the laser-cut edge was studied. As shown in Fig. 26, a better edge cut was achieved when cutting with argon at higher power. Surface roughness was maximum when using oxygen and minimum with argon. HAZ was minimum with nitrogen and maximum with oxygen due to its exothermic chemical reaction. Argon is preferable for dross free cutting. Kerf width was found to be minimum in argon and maximum in air.

3.4.3. *Other fluid-assisted LBM*

The researchers also tried to perform fluid-assisted LBM with fluids other than water. **Hwang** et al. fabricated a high aspect ratio

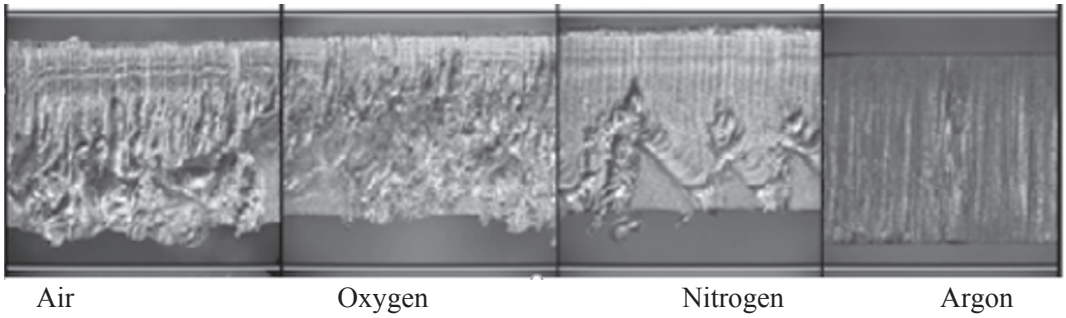

Fig. 26. Surface morphology of cut edge of samples processed by different gas [104]. [Reproduced by permission of the publisher. Permission to reuse must be obtained from the rights holder].

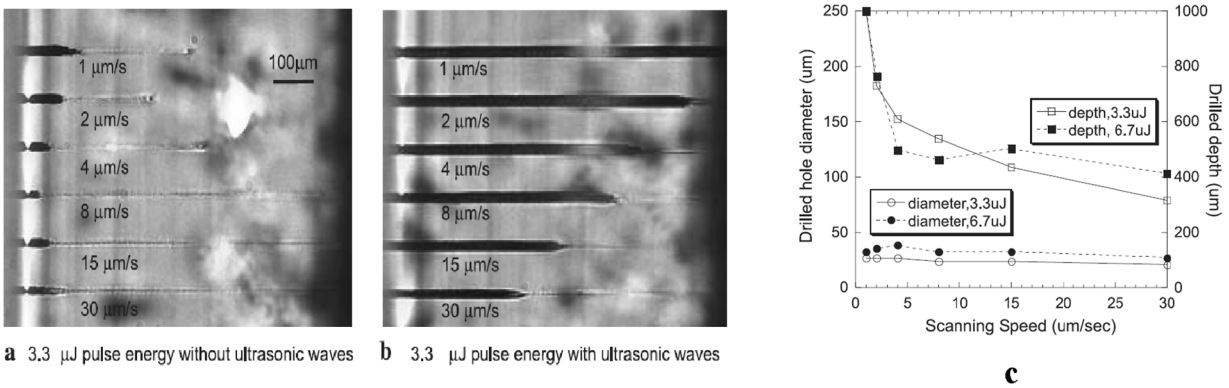

Fig. 27. Measured depth and diameter of drilled hole corresponding to the holes [105]. [Reproduced by permission of the publisher. Permission to reuse must be obtained from the rights holder].

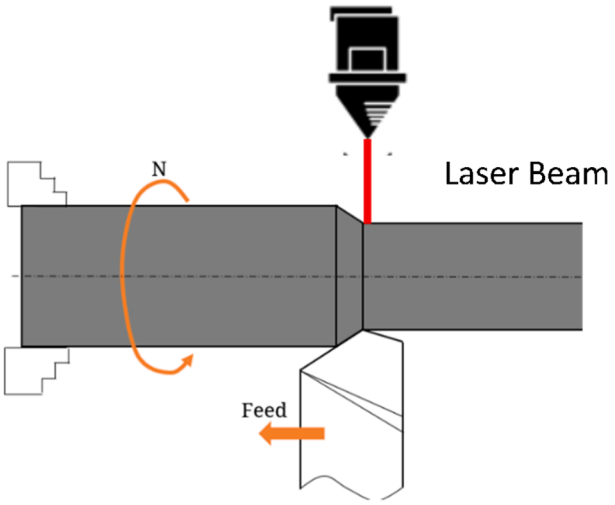

Fig. 28. Setup laser-assisted turning [109].

microchannel on 1.25 mm-thick optical glass by liquid-assisted fs laser machining [105]. A femtosecond laser of 800-nm wavelength with pulse energies ranging from 3 to 33 μJ was used for experimentation. No post-machining and treatment of the channel is required. Straight channel drilling was done at different scanning speeds in air, methanol, distilled water, and isopropanol alcohol. The machined channel appeared bright when liquid assisted machining was done and appeared dark in absence. Distilled water and methanol assisted drilled hole was deeper, and an in *iso*-propane assistance hole was non-uniform. Ultrasonic waves improved the aspect ratio up to 40:1 while the diameter uniformity also improved, as shown in Fig. 27. 3D channel, bent holes, and the curved channel were also fabricated on glass and found low viscosity liquid to be more effective for removing debris. The heating of liquids decreased viscosity, which was preferable for effective material removal.

Posa et al. performed Experimental laser micro machining using 40 W CO_2 Laser on Borosilicate Glass with a chemical mixture of ethyl acetate, silica, camphor, and aluminium borosilicate. Results show two times increase in width of the slot, four times increase in depth of the slot, and seven times increase in material removal rate (MRR) on an average [162].

The above studies conclude that assist gas aids in improving the machining process for metal removal and a significant surface quality improvement. Inert gases can also be chosen for a high surface finish. However, air or oxygen is preferred for exothermic assistance in the removal mechanism of melting and vaporization.

4. Assisted machining with laser as secondary process

In this section of the article, the laser beam processes assisting other micromachining processes such as turning, milling, ECM, and EDM are reviewed. Previously, researchers also termed it hot machining. Development of such processes will be benefitted by faster machining to improve production capacity in industrial applications. A significant reduction in cutting forces and tool wear is observed in turning and milling. However, laser heating improves MRR in ECM and EDM processes.

4.1. *Laser-assisted turning process*

Laser-assisted turning is used to machine difficult to machine material by combining laser beam and conventional single-point turning tools for cylindrical workpieces. Here, the laser beam assists machining, acting as a secondary process, and primary machining was carried out with a turning tool [106,107]. It has an application to reduce the diameter of the circular part. In laser-assisted turning, the laser beam energy is utilized to heat circular rotating workpiece, and interaction between tool and workpiece causes removal of material [109]. The workpiece softens and becomes ductile, and there is a significant decrease in cutting forces. The laser beam is incident perpendicular or at an angle on a rotary workpiece, as illustrated in Fig. 28. Although there is a need to optimize the optimum cutting power of laser beam. Higher power may cause thermal cracks and poor surface integrity [160].

Wang et al. performed laser-assisted micro-turning of Al_2O_3 reinforced particle aluminium matrix composite using 150 W Nd: Yag laser and carbide turning tool [110]. Radial force Fy and axial force Fx reduced by 50%, and main cutting force Fz reduced by 10%, as depicted in Fig. 29. Tool wear was analyzed by studying the change in effective tool diameter due to softening of the workpiece, which further reduces the push forces of Al_2O_3 particle on composite on the tool's clearance face, so a significant reduction was observed.

Panjehpour et al. performed LAT of AISI52100 steel and focussed on the impacts of average power, pulse repetition rate, pulse energy, cutting velocity and feed rate on MRR, temperature, specific cutting energy, surface finish, microstructure, tool wear rate, and chip formation [111]. Nd: Yag laser was utilized for machining, and cutting force was measured by strain gauge sensor. A non-contact type infrared camera also measured the temperature. A regression model was

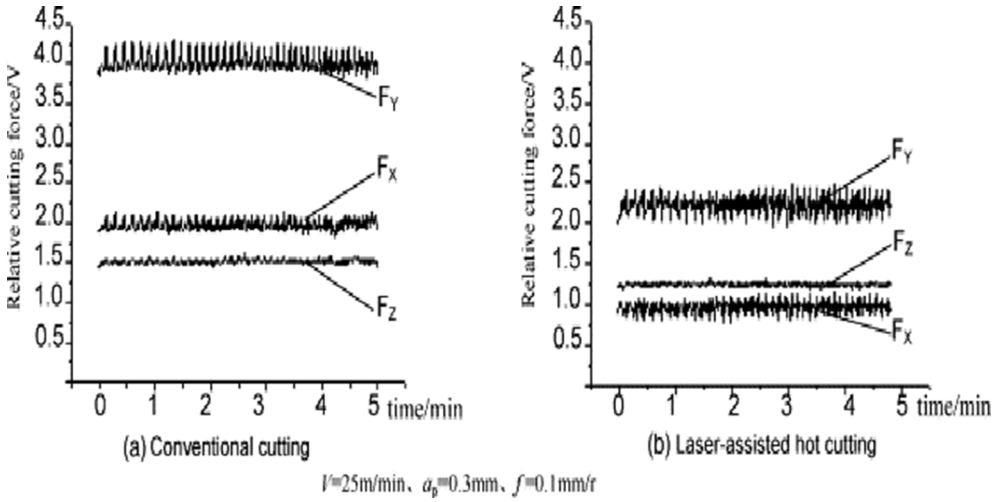

Fig. 29. Comparison of cutting force in conventional and assisted cutting [110]. [Reproduced by permission of the publisher. Permission to reuse must be obtained from the rights holder].

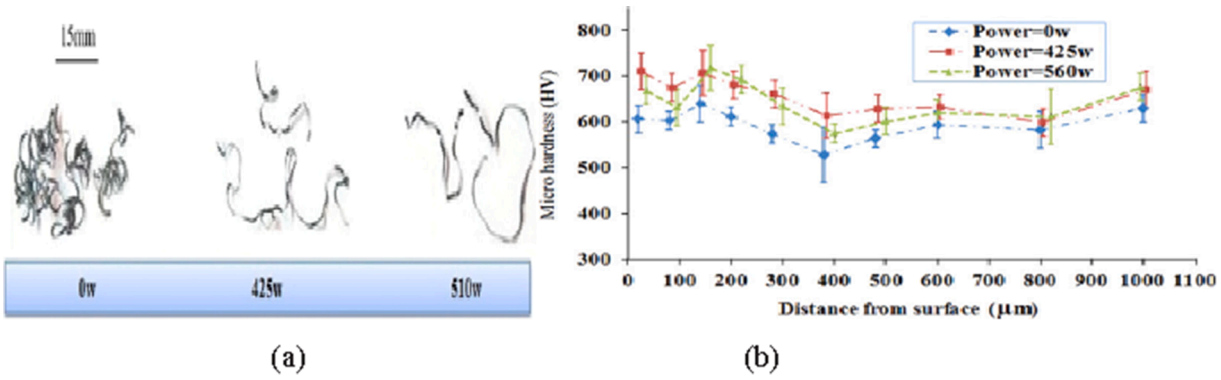

Fig. 30. Chip morphology at different power and microhardness [111]. [Reproduced by permission of the publisher. Permission to reuse must be obtained from the rights holder].

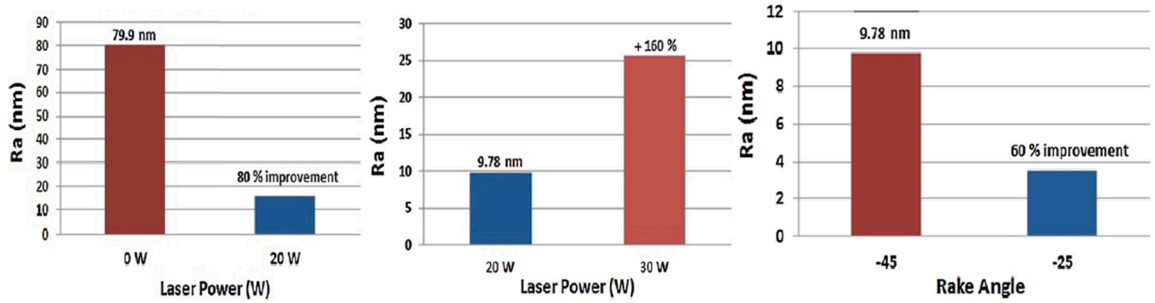

Fig. 31. Comparison of surface roughness with laser power and rake angle [112]. [Reproduced by permission of the publisher. Permission to reuse must be obtained from the rights holder].

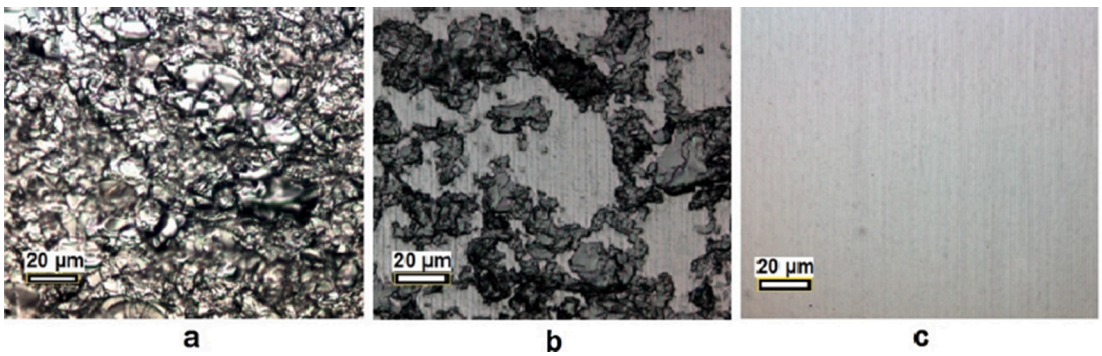

Fig. 32. (a) Unmachined surface (b) conventional method machined (c) LAM machined [112]. [Reproduced by permission of the publisher. Permission to reuse must be obtained from the rights holder].

developed for temperature based on the experiment. In LAT, specific cutting energy was reduced by 25%, while the temperature and surface roughness also lowered for LAT compared to conventional turning. LAT-produced chips are continuous, and by an increase in power, its curvature also increased, which shows the thermal softening effect as exhibited in Fig. 30 (a). LAT further increases the microhardness of the surface, which is due to severe plastic deformation, as shown in Fig. 30 (b) [111].

Single point diamond tool (SPDT) assisted by micro-laser machining on silicon with cutting fluid performed by **Mohammadia et al.** [112] using IR CW laser. They considered laser parameters (laser power) and SPDT parameters (cross–feed rates and rake angle) to analyze the effect on surface roughness. The laser beam was delivered through the cutting tool and aligned with the tool with beam delivery optics. LAM setup was mounted on a precise diamond turning machine [112]. In roughing pass, roughness increased by 80% with laser assistance as compared to without laser assistance. This was due to a significant reduction in pull out resulting in a better surface, and due to laser heating, the ductility increased of the machining region. High negative rake angle caused rubbing of surfaces. So poor surface finish was achieved, as illustrated in Fig. 31. Optimum laser power needs to be selected deliberately so surface roughness does not increase drastically. Overheating causes thermal cracks, and material flows to the side of the tool nose and built-up. The ductile mode of machining causes better surface finishes in LA SPDT, as shown in Fig. 32.

Silicon has poor machinability due to its brittle nature. Mechanism of ductile mode machining of silicon by high-pressure phase transformation (HPPT) with LAM was investigated by **Ravindra** et al. [113] by infrared (IR) diode laser. A tool was developed to supply laser beam along rake angle to heat workpiece surface, as shown in Fig. 33. Optimum power condition resulted in the deepest cut and getting the surface as the original. Process characterization was established for cutting and

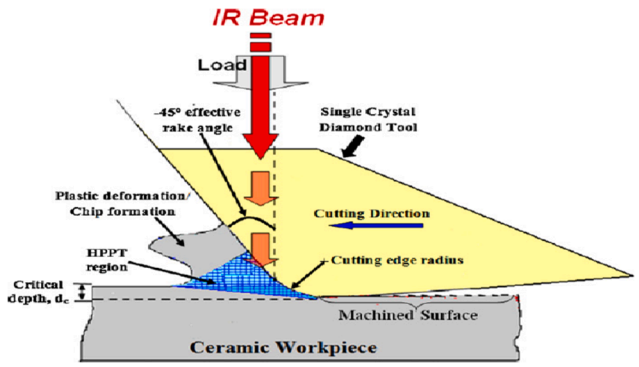

Fig. 33. Schematic of the HPPT region at the tool-workpiece during LAT [113]. [Reproduced by permission of the publisher. Permission to reuse must be obtained from the rights holder].

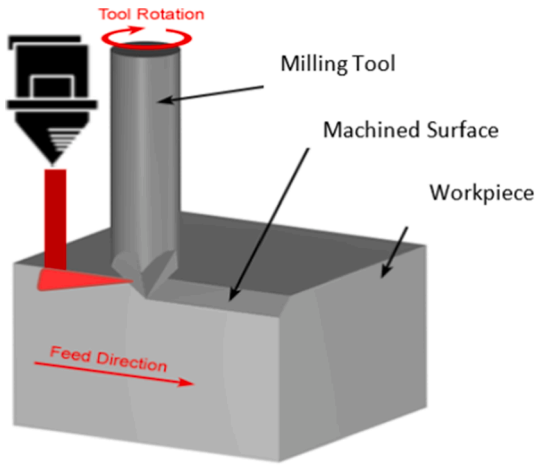

Fig. 34. Schematic of laser-assisted milling [118].

thrust forces considering parameters laser power, cutting velocity, rake angle edge radius [113].

Cutting force reduced by 60% while machining Inconel 718 by LAT in the study carried out by **Venkatesan et al.** [114]. From the result, they recommended work surface temperature in the range between 750 and 880 °C during LA turning of Inconel for maximum force reduction. They analyzed the contribution of laser power for cutting force and found reduction by 19%, 26%, and 53% in feed force, thrust force, and cutting force, respectively.

Optimization of LAT for conventional turning and laser parameters was performed experimentally and numerically by **Ayed et al.** [115]. The developed cutting model understood the mechanism of chip formation. Significant cutting force reduction was reported due to cutting conditions and laser characteristics.

Researchers are also working on modelling the process to analyze the mechanism and understanding. A 3D longitudinal and orthogonal turning FEA model was developed to observe the effect of laser power, cutting velocity, and rake angle on cutting edge radius and thrust force for LAM of AISI D2 tool steel turning by **Singh et al**. [116]. They observed a 30% reduction in flow stress with laser assistance.

LAT is successfully employed in different ways to improve process capability and improvement in product quality. Tool life and surface quality improvement, and reduction in cutting force are significant attributes of the process compared to the conventional method.

4.2. *Laser-assisted milling process*

Micro milling technique can produce 3D surfaces of the smallest feature size, 10 μm, with rotary micro end mills at 50,000 RPM or more. The physical cutting process leads to cutting forces, and material removal depend on uncut chip thickness. Micro end mills typically lead to failure by complete fracture [117]. In the LAM laser beam, preheat the workpiece at a location just ahead of micro end mills, as shown in Fig. 34. Preheating before machining softens the workpiece and degrades the workpiece's mechanical property reducing cutting forces [118–120]. LAM process is shown improvement in tool life and surface characteristics [161].

Lahoti et al. developed a four-axis LAMM machining system to perform machining of a tool steel (62 HRC). A relatively low power (max. 35 W) Ytterbium-doped continuous wave near IR (1.06 mm) fiber laser is used for machining. No assist gas is used. Machined microgroove's surface finish and dimensional accuracy were superior over the cutting distance in LA micro-milling with minor tool wear. In surface roughness, profile consistency was achieved with laser assistance [121]. In Fig. 35, surface roughness shows the inverse response with laser assistance when contrasted with traditional machining and appeared improvement with cutting speed, although groove depth accuracy improved.

Two new laser machining parameters, i.e., laser angle and laser power, were introduced for laser-assisted machining by **Venkatesan et al.,** and optimization of the process cutting force and temperature for Inconel alloy was carried out [122]. Nd: YAG laser source with maximum 2 kW power used for machining and empirical equation was also produced. Improvement in tool life was found to be 43% in LAM as compared to without assistance. In LAM assisted machining, reduction of 34%, 34%, and 38% in cutting forces in X, Y, and Z direction were found compared to conventional machining, as evident in Fig. 36(a). Fig. 36(b) shows that the tool wear rate was at least six times

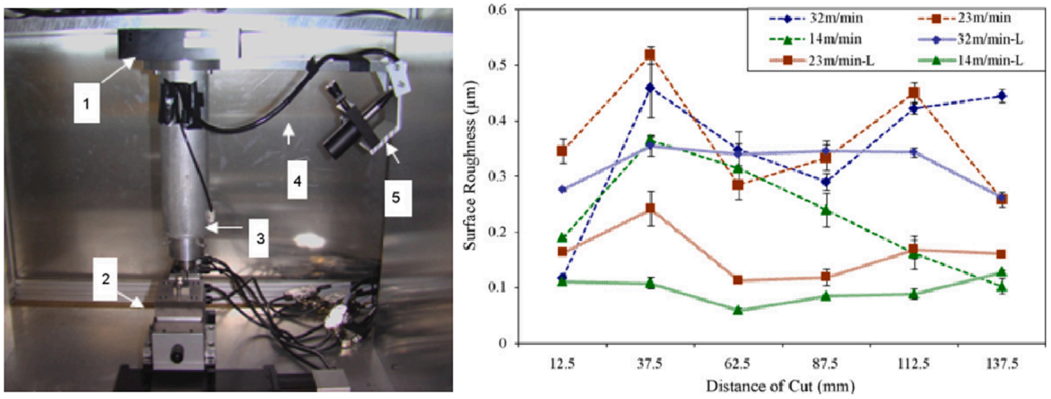

Fig. 35. (a) Experimental setup, (b) Surface roughness variation with cutting distance for different cutting speeds [121]. [Reproduced by permission of the publisher. Permission to reuse must be obtained from the rights holder].

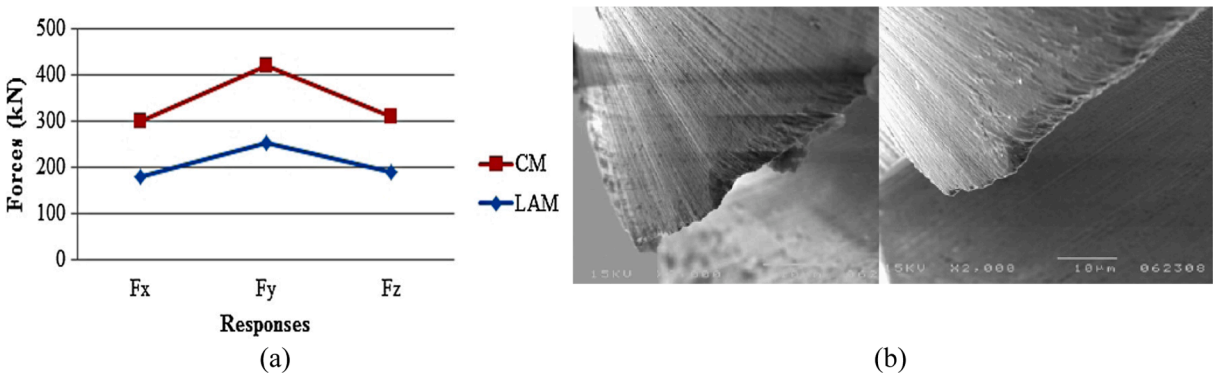

Fig. 36. (a) Force comparison in conventional and LAM, (b) tool wear comparison between conventional tool after 5.5 min and LAMM tool after 33 min of machining [122]. [Reproduced by permission of the publisher. Permission to reuse must be obtained from the rights holder].

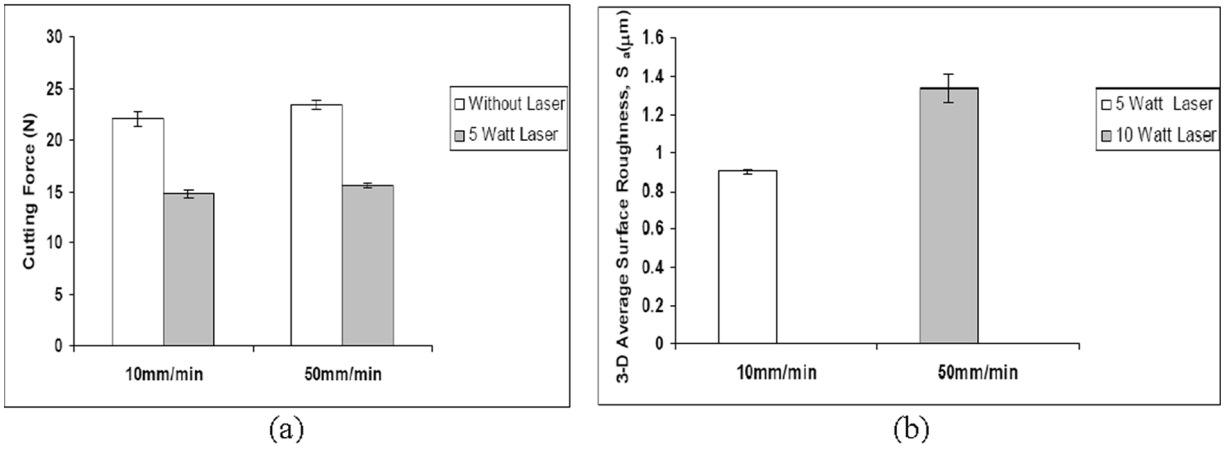

Fig. 37. (a) Cutting force with and without laser power, (b) Surface roughness variation with different laser power [123]. [Reproduced by permission of the publisher. Permission to reuse must be obtained from the rights holder].

conventional machining compared to LAMM for stainless steel. For In718 and Ti alloy, there was no significant reduction in tool wear observed, which may require a wide range of experiments.

The effect of laser parameters and cutting parameters while doing LAM on H-13 tool steel was studied by **Singh et al.,** and cutting forces and surface finish were analyzed for micro grooving applications [123]. A 2–10 W solid-state Ytterbium fiber laser is integrated with a precision 2-axis motion control stage. Thermal softening causes a significant reduction in cutting forces and increases surface roughness, as shown in Fig. 37(a). An increase of 48% in roughness was observed when laser power increased from 5 W to 10 W, although cutting speed was different, as exhibited in Fig. 37(b). The temperature profile between the work material and the cutting tool demonstrates the most extreme temperature at the laser beam centre.

Kumar et al. looked for potential in laser-assisted micro-milling process in the manner of cutting force, tool wear, MRR, surface finish, and burr formation [153]. A 35 W CW fiber laser (1.06 μm wavelength) is used for thermal machining. There were 69% lesser cutting forces observed in LAMM than traditional micro-milling, as depicted in Fig. 38 (a). Also, catastrophic failure of the tool was observed in a significantly earlier stage without laser assistance. One more crucial observation was found in the tool's corner radius; it is extensively smaller than conventional micro-milling in LAMM. Gradual wear was observed while using non-laser-assisted machining, which indicated rounding of the cutting tool's corner due to abrasive wear, as illustrated in Fig. 38(c).

It was also observed without laser-assisted machining, the groove profile changed significantly due to rapid tool wear. The depth observed in laser-assisted milling was higher as compared to without laser assistance. Burr height was also primarily because of increment in ductility by softening workpiece in laser assistance, as evident in Fig. 38 (b). Surface roughness depends on the spot size of the laser beam. Surface roughness increases if the laser spot diameter is more than tool diameter in LAMM due to thermal softening consequences.

A finite Element Analysis (FEA) based thermal model on anticipating the width and depth of HAZ in LAM was developed by **Yang et al.** [124]. A 2.5 kW Nd: YAG laser system was utilized to generate a laser beam. A thermal model was developed to predict the width and depth of HAZ, which depends on laser parameters and material properties. A travelling laser source having a Gaussian profile was considered in FEA for laser assisting machining of Ti6Al4V. The absorptivity and emissivity of the Ti alloy were determined by measuring temperature with a thermocouple. Predepicted value of width and depth of HAZ showed closeness to measured.

HAZ dimensions were predicted in LAMM in another study for micro grooving operation H-13 tool steel with 10 W power at different scanning speeds [125]. The authors have developed a set-up for micro grooving operation, as shown in Fig. 39(a). FEA model developed for moving Gaussian laser beam to predict temperature distribution. The thermocouples were used to observe maximum temperature when the laser beam nearest to it. Simulated and experimental results were compared at different scanning speeds for temperature, which predicted HAZ and temperature within 15% accuracy, as evident in Fig. 39(b).

In the laser-assisted machining process, optimum parameters are needed for both machining processes, i.e., laser and cutting processes. **Tagliaferriet et al.** optimize process parameters of laser for HAZ extension, track width, temperature. Laser power and scanning velocity

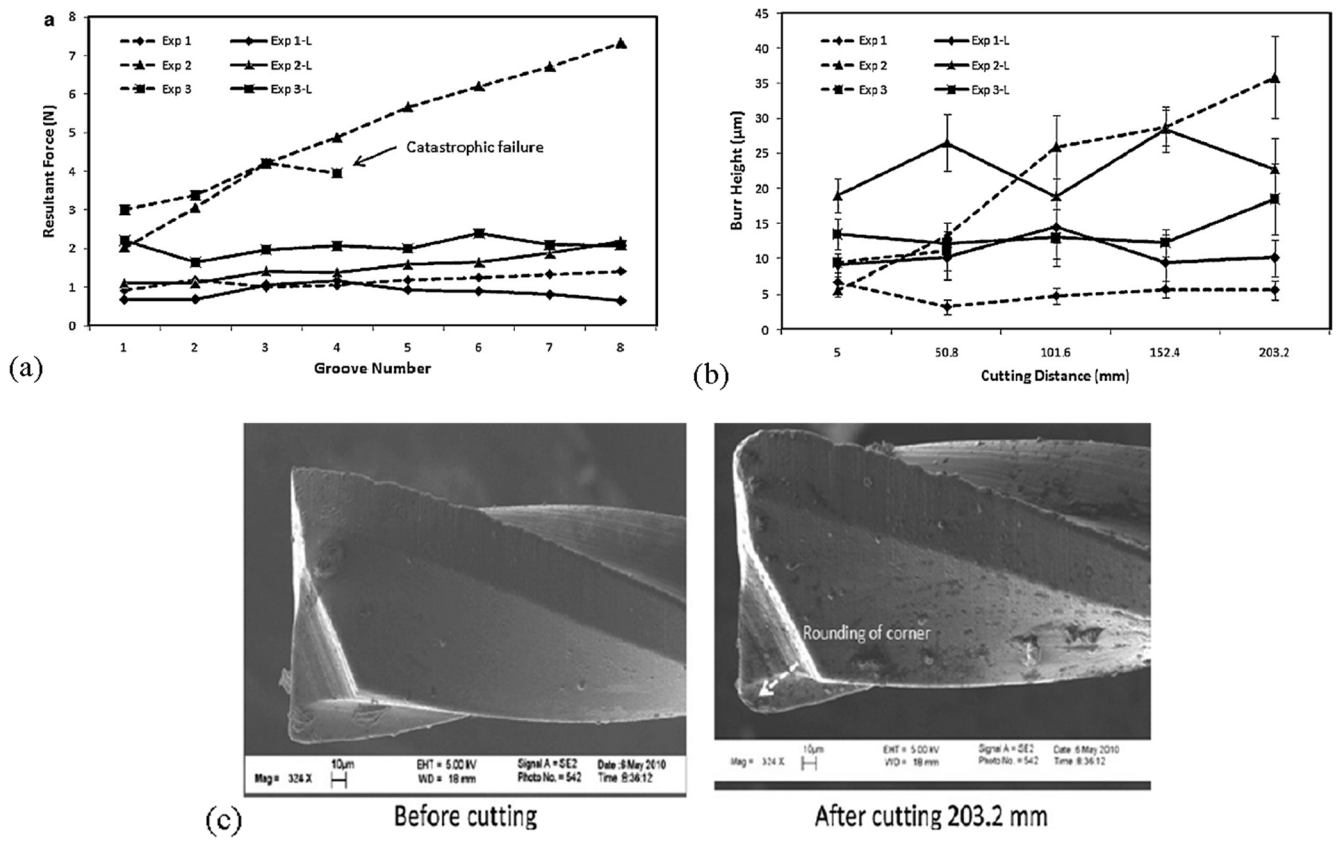

Fig. 38. (a) Changes in the maximum resultant force with groove number (b) Burr height versus cutting distance (c) SEM micrographs of the tool before and after cutting [153]. [Reproduced by permission of the publisher. Permission to reuse must be obtained from the rights holder].

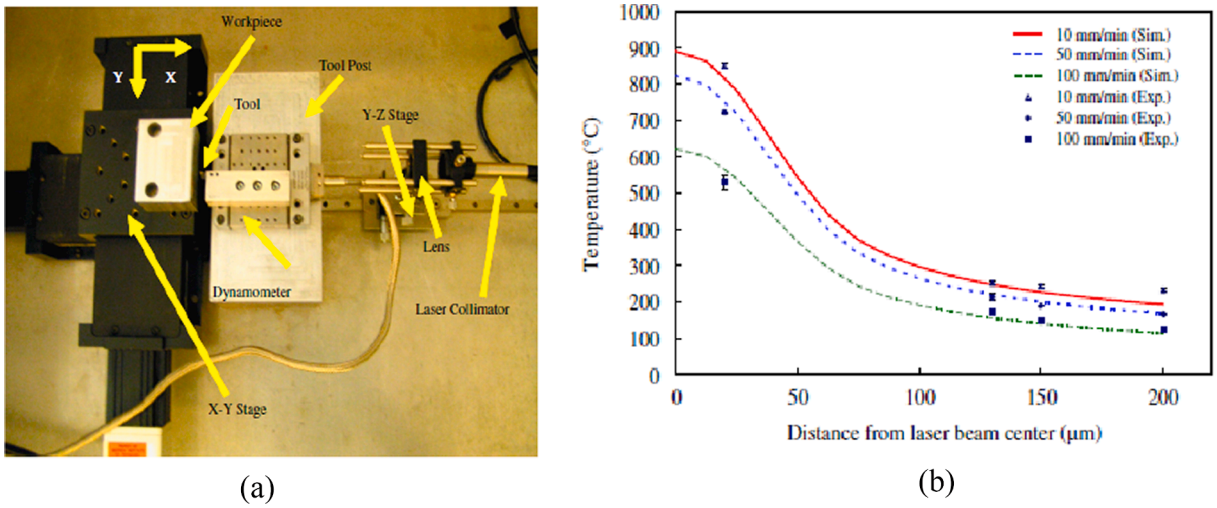

Fig. 39. (a) LAMM setup (b) Simulation and experimental results for 5 W laser power [125]. [Reproduced by permission of the publisher. Permission to reuse must be obtained from the rights holder].

had a strong influence on LAM. They observed that laser power and scanning velocity have significant effects compared to other factors, defocus and surface quality [126].

Bucciarelli et al. compared the machineability of A-286 steel in dry, wet, with and without laser-assisted micro-milling conditions [127]. A Ytterbium-doped continuous wave fiber laser (IPG Photonics – YLM 30) with a Gaussian beam of 1070 nm nominal wavelength is focused on a diameter spot of 300 μm. They observed a decrease in tool wear rate by 29% compared to wet micro-milling with LAMM. An average of 10% cutting force was also reduced in dry conditions in LAMM machining. An average 10% reduction in cutting force was observed in dry LAMM machining. Precise and uniform groove geometry was observed during LAMM. Fig. 40 shows the quality of channel produced by LAMM is better than wet and dry condition; however, at higher power burr is more due to softening of the material

Ahn et al. compared the specific energy requirement for LAM and CMM by tangential force and MRR. It is observed lower with different feed and rotational speed values.[109]. At a depth of cut of 0.2 mm, the

Fig. 40. Comparison of surface quality in dry and wet conditions [127]. [Reproduced by permission of the publisher. Permission to reuse must be obtained from the rights holder].

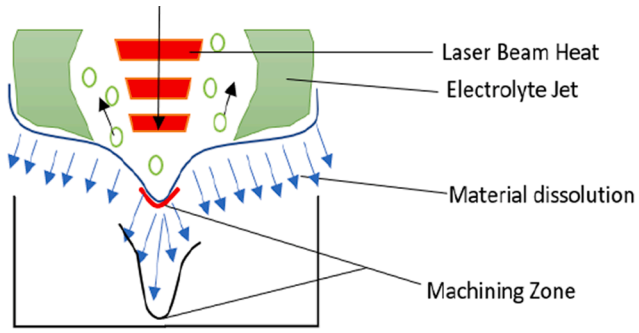

Fig. 41. LAJECM process mechanism [128].

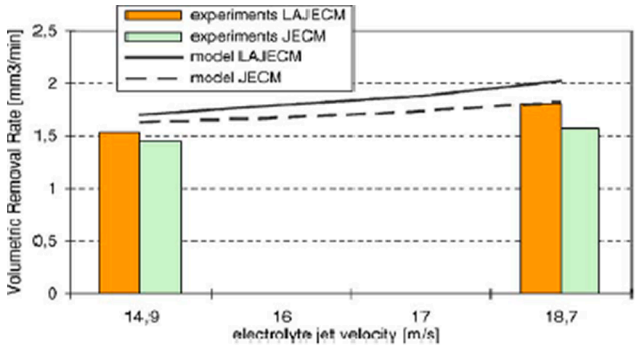

Fig. 42. Comparison of LAJECM and JECM [128]. [Reproduced by permission of the publisher. Permission to reuse must be obtained from the rights holder].

specific cutting energy of LAM decreased by a maximum of 60%. Radial force and tangential force is observed significant lower in the LAM method.

Different scholars tried to develop LAM in the lab and studied its attributes on tools and workpieces. Modelling of cutting force, tool wear, surface roughness and MRR were also covered in past studies. Comparative analysis shows process improvement in process efficiency with laser assistance to micro-milling.

4.3. Laser-assisted electro-chemical machining

In laser-assisted ECM, both processes are combined to overcome the limitation of each other. In ECM, precision is limited, and in LBM, thermal stress causes defects. In laser-assisted electrochemical machining (LAECM), two different principles remove the material simultaneously in which LBM works on the energy of photons while ECM has ions energy, as shown in Fig. 41. Electrolyte sent in the form of the jet supplied co-axially with the laser beam reduces the recast layer in laser drilling. Laser-assisted jet ECM(LAJECM) is popular for precise

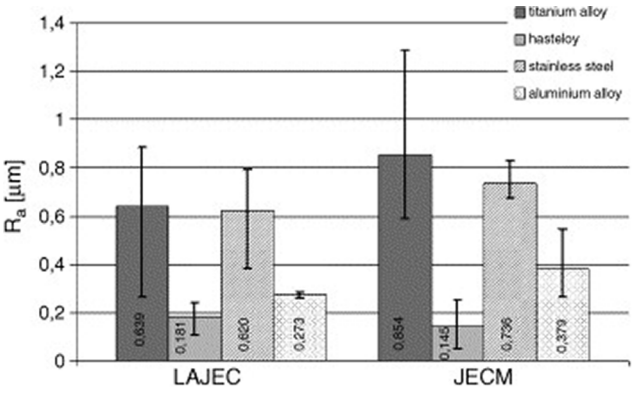

Fig. 43. Comparison of LAJECM and JECM for different material [129]. [Reproduced by permission of the publisher. Permission to reuse must be obtained from the rights holder].

machining holes with faster speed. LAJECM is a hybrid process in which LBM and ECM's combined effect will improve machining quality and high precision. ECM is a well-established process and has many applications because of no thermal stress and surface defects. A low power laser beam is combined co-axially with an electrolyte jet for localized heating in LAJECM for noncontact machining.

Pajak et al. developed a setup for LAJECM in which laser beam and electrolyte emerge from a nozzle of 0.1 mm diameter. The laser (power density 47.5 W/mm^2) is used for hybrid machining. Electrolyte jet energy, laser beam energy, and electrolyte flow energy are balanced for causes of electrochemical dissolution [128]. They developed an empirical model to compare MRR and taper for JECM and LAJECM considering variable inter-electrode gaps, voltage, flow velocity, and electrolyte concentration. Results show taperness decreased by 40%, and MRR increased by 55% in hole drilling of silicon, as shown in Fig. 42.

In another study, LAJECM was performed to machining Hastelloy, titanium, stainless steel (SS), and aluminium. The result showed improvement in MRR 20%,25%, 33%, and 54% and taper reduction 38%, 40%, 41%, and 65% respectively. In LAJECM, laser beam energy makes the hole-making process faster regardless of the JECM process variable [129]. Titanium and oxygen form TiO_2, so laser beam breaks the layer more quickly than JECM, and improvement in MRR was observed in Hastelloy and SS machining. Roughness result shows up to 25% improvement in LAJECM compared to JECM for all materials shown in Fig. 43.

A theoretical model for the explanation of the effect of localization of electrochemical dissolution in the LAJECM process was developed by **Silva et al.** [130]. The combined effect of laser beam energy and electrolyte jet energy causes the dissolution of material in the machined area. Theoretically, energy distribution was calculated for different

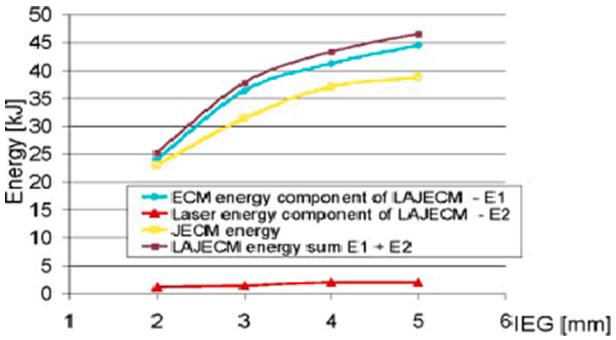

Fig. 44. Process energy for aluminium alloy, U = 140 V, C = l0% [130]. [Reproduced by permission of the publisher. Permission to reuse must be obtained from the rights holder].

inter-electrode gaps (IEG) for aluminium and found LAJECM have higher energy than JECM, as exhibited in Fig. 44.

Zhang et al. performed LAJECM for drilling on stainless steel of 0.5 mm thickness by two different lasers, 1064 nm and 532 nm. Fig. 45 (a, b) shows the difference in the mechanism of machining of LBM and LAJEM principle for surface appearance of blind holes [131]. From Fig. 45 (c, d), it has been observed there is no spattering and recast around the hole periphery in LAJECM. However, laser drilling in the air shows spatters and recast. MRR efficiency in ns LBM is 50% higher than jet electrochemical laser drilling (JECM-LD) shown in Fig. 45(e).

In another study, the temperature distribution in w/p and IEG analyzed for localized heating with FEA modelling was done [70]. In the laser localized heating zone, the temperature was 1.75–3.25 times higher than the electrolyte temperature in different metals depicted in Fig. 46. Temperature decreased with an increase in thermal conductivity of metal of localized heating zone. Temperature above 100 °C was a cause of bubble formation in the electrolyte. Higher the temperature of the localized zone causes higher MRR. Temperature first increases and get stable, then decreases, which shows heating leading to boiling than stable machining and closure of machining.

Wang et al. proposed a novel approach of hybrid laser and shaped tube electrochemical machining process. Both the laser beam and electrolyte jet are guided to the machining zone through the inner hole of a specially designed tubular electrode. The laser beam is reflected many times in the tube to reach the machining zone to achieve the combined effect of ECM and LBM to fabricate high aspect ratio holes. Results showed that the machining precision and the material removal rate (MRR) were improved by 60.7% and 122.7%, respectively, compared with that pure ECM. Experimental results showed electric current increased from 0.7 to 1.08A with the laser power of 20 W, an increase of 54.3%, compared with that without laser [158].

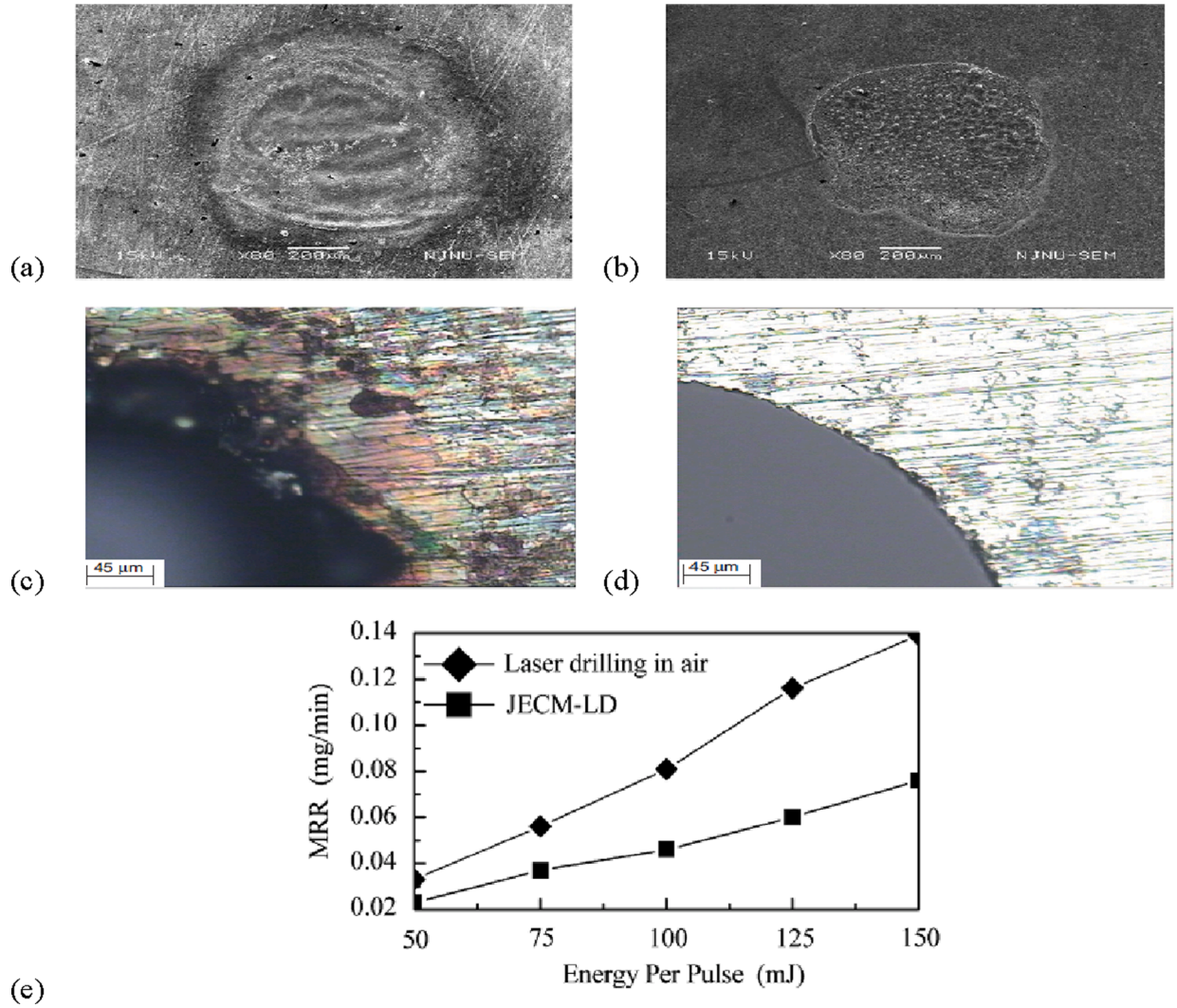

Fig. 45. Comparison in the mechanism for the blind hole (a) LBM (b) JECM-LD; Micrograph of the periphery drilled hole (d) LBM (d) JECM-LD (e) Effect of energy per pulse on MRR [131]. [Reproduced by permission of the publisher. Permission to reuse must be obtained from the rights holder].

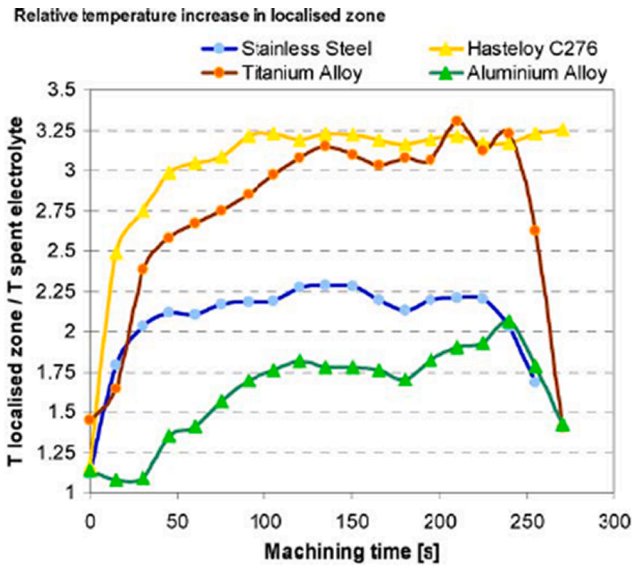

Fig. 46. Temperature in the laser localized zone and electrolyte with machining time [70]. [Reproduced by permission of the publisher. Permission to reuse must be obtained from the rights holder].

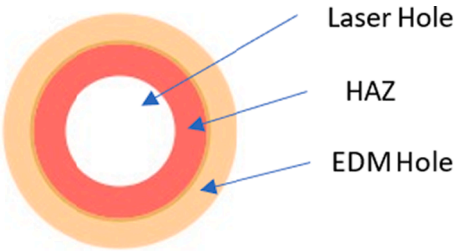

Fig. 47. Sequential laser and EDM performed [132].

Previous studies concluded laser assistance to the ECM process improves MRR and machining efficiency. However, the process is limited to an electrically conductive material. Researchers also model the hybrid process to understand the interaction of the hybrid process. Further experimentation is needed for the industrial application of the process for highly precise parts.

5. Laser-based sequential machining processes

This section reviews the hybrid process in which laser machining is used sequentially with the process such as EDM, conventional drilling and milling. However, in this decade, these processes still need to be explored by researchers in more depth. Here laser machining is used for the primary machining of holes, micro-grooves and predefined shapes. Final geometry and surfaces will be the result of the secondary machining process.

5.1. Sequential LBM and EDM machining processes

At present, researchers are continuously working on combining LBM and EDM processes. The hybrid process can fabricate highly precise holes, channels, cut sheets and create 3D geometries. The combined effect of both the process has been analyzed and demonstrated by researchers. The laser acts as a faster machining process in the hybrid process; however, EDM produces a high finish surface. In EDM, the cost of hole making getting higher due to the breakage of electrodes and lower MRR. However, the industrial standard hole cannot achieve in LBD due to larger recast and heat-affected zones except ps and fs laser.

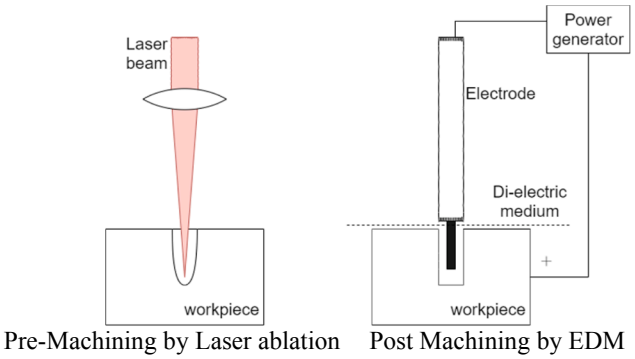

Fig. 48. Sequential LBM AND EDM machining method [133].

So the sequential process is alternate for higher efficiency machining.

Li et al. performed LBM and EDM sequentially in application hole micro-drilling for fuel injection nozzles. An Nd: YAG laser (1064 nm wavelength) with 10–40 μs pulse length at a repetition rate of up 2000 Hz with 15 mJ/pulse for drilling pilot holes. A pilot hole of 140 μm diameter was drilled by laser and sequentially rimmed by the EDM process. The authors also replaced the standard EDM electrode dressing, which takes 4 s, with a new online cutting to dress the tool between machining of each hole, which took 1 s. Process schematic is shown in Fig. 47. Drilling time also improved by 70% in the sequential process than EDM drilling alone [132]. They also claimed that this technique reduced the cost by 42% (excluding the initial capital investment) and increased the production capacity by 90%. EDM also removed the problem of HAZ and recast layer after LBM drilling. It is also pertinent to note that both machining processes (LBM and EDM) directly engaged in removing the material from the machined parts in this hybrid technique.

LBM and EDM were combined to get faster machining with LBM and finishing by EDM to improve the surface quality and MRR further. **Rashid et al**. analyzed the combined process effect on HAZ, surface quality, machining time, and material composition. A 100 W fiber laser carried out primary machining. They concluded that surface roughness after LBM was 1.54 μm and, after sequentially applying EDM, reduced further to 0.23 to 0.28 μm at different feed rates [133]. The chemical composition of the workpiece also severely affects the machined zone. It was observed that carbon content decreased after EDM, while oxygen content increased after the laser process but decreased to the original after the EDM process.

Kim et al. performed sequential machining of LBM and EDM to allow faster machining and reduce tool wear for conductive materials [134]. A Yb-doped pulsed fiber laser (wavelength 1064 nm) with a pulse length of 100 ns was used in the experiment for laser ablation. Pre machining is performed by laser ablation and post-machining by EDM in dielectric fluid, as shown in Fig. 48. The machining was performed on the same machine, and the workpiece travelled by XY stage to two different machining processes, i.e., first to ns pulsed laser and then to microwire EDM. The hole quality characteristics were enhanced after EDM, which had a considerable amount of recast layer during laser ablation. Machining time was reduced to halves in the sequential method, and tool wear showed only 12% improvement. Laser predrilled holes made uncomplicated debris removal and the machining rate was higher than standard EDM drilling. Micro grooves were also created using the hybrid process of laser pre deburring and post EDM. A perfect U-shaped microchannel requires a vertical wall, which was fabricated by the sequential method. As laser-produced less HAZ with high aspect ratio but introduced V shape channel. 3D geometries, such as a micro pyramid, hemisphere, snail-shape, and circular were also tried without additional polishing.

Ahmari et al. performed hybrid machining with LBM and EDM. A pilot hole was fabricated by laser drilling, and the pilot hole was finished by EDM [135]. The laser machining setup of Nd: YAG laser operating at

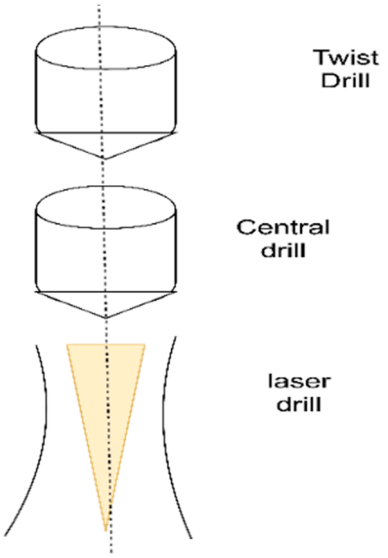

Fig. 49. Sequential laser and conventional drilling [74].

a wavelength of 1064 nm. Both processes were performed on two different machines. Compared to EDM, the hybrid process showed a 50–65% faster machining rate. The pilot hole was drilled by laser drilling, and then another setup of RC circuit based EDM was utilized for further machining and investigation. In the hybrid process, the hole is straight, and debris particles do not promote machining as through pilot hole dielectric and debris flows out of the hole. Hole quality is poor in laser machining. High MRR, lower taper, and lower overcut were observed in LEDM, which benefited from the hybrid process.

Rashid et al. performed the LBMM-μ-EDM-based sequential micro-machining process. Results show 2.65 times lesser production time for holes compared to EDM [159]. High tool wear rate and short circuit rate were observed during the μ-EDM operation if low laser power and high scanning speed were used for the LBMed holes.

Researchers successfully employed Sequential LBM and EDM to fabricate high-quality micro-holes and channels. A machining setup needs to be developed for the combined process to avoid alignment errors.

5.2. Sequential LBM and conventional micro-drilling

Laser micro-drilling suffers from drawbacks of roundness error, taperness, spatter and lower aspect ratio. However, conventional micro-drilling suffers from high tool wear, cutting forces, and higher tooling costs. Researchers combined these processes for high-quality hole fabrication on different materials. LBD process drills a primary hole, and the final dimension of the hole is achieved by the drilling tool with lesser forces.

Okasha et al. performed micro-drilling on Inconel 718 sequentially by laser and conventional micro tools at a 30° acute angle. In pilot laser hole drilling, oxygen and air were used as assist gases [136]. Post laser drilling, the micro-drilling technique finished the hole. They observed minimal burr and no wall destruction when performed LBM through holes drilling with air as assist gas followed by mechanical drilling compared to a mechanically drilled hole. Tool life also showed 2.5X improvement in the sequential process when compared to the traditional drilling process. Air assistance shows 1.5 times faster machining than oxygen in the same laser cutting condition because of the formation of oxides.

In another study, a sequential LBM-drilling process to drill 500 μm holes on a 2 mm sheet of Inconel 718 was done by two approaches [74]. The pilot hole was drilled in the first approach using a laser followed by a mechanical twist drill. In the second approach, drilling was performed in three steps, i.e., laser pilot drilling followed by mechanical central drilling and then twist drilling, as shown in Fig. 49. Laser pilot drilled in range of 391–450 μm. The laser pilot-mechanical drilling technique reduced thrust force by 57% and 37% in a two-step and three-step approach. Laser drilled holes were found to be inferior in roundness in both approaches. However, the roundness of the laser pilot-mech hole is similar to conventional mechanical drilled holes. The tool life showed a significant improvement in both the laser-mech and laser pilot mech approaches. A single tool in conventional, laser-mech, and laser pilot mech methods can drill 106, 304, and 458 holes, respectively.

The above studies conclude that drilling can be accomplished with sequential laser and drilling tools. Improvement in tool life and circularity of holes and reduction in cutting force are significant benefits.

5.3. Sequential LBM and conventional micro milling

As discussed in the above section, hole making, highly finished microchannels, micro-grooves, and precise shape can be achieved using a sequential laser and micro-milling tool. In Laser milling processes, recrystallization of material occurs due to heating and oxidation, which results in the variation of material property. To achieve material property as original, sequential LBM and conventional micro-milling is utilized by the researcher. The fundamental difference is to use the laser's heat energy to soften the metal, and heated metal gets removed by tool motion. The cutting stress developed due to the removal of material is lesser than CMM, which leads to reduced forces. The milling tool follows the laser beam path, and heat-affected material gets removed in ductile mode due to melting.

The manufacturing of hot embossing dies have limitations such as accuracy, surface integrity, material properties, and size $<$ 100 μm.

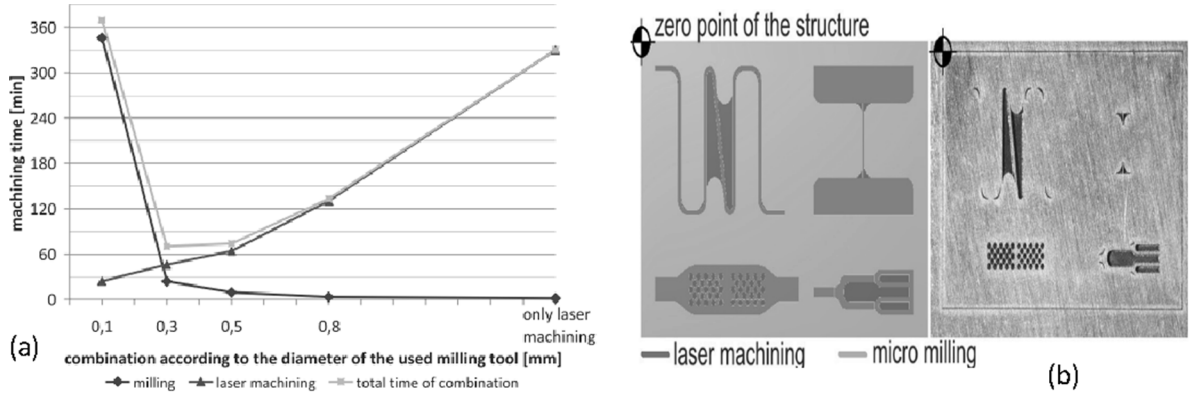

Fig. 50. (a) Machining time in hybrid machining (b) 3D structure fabricated by sequential laser and conventional machining [137]. [Reproduced by permission of the publisher. Permission to reuse must be obtained from the rights holder].

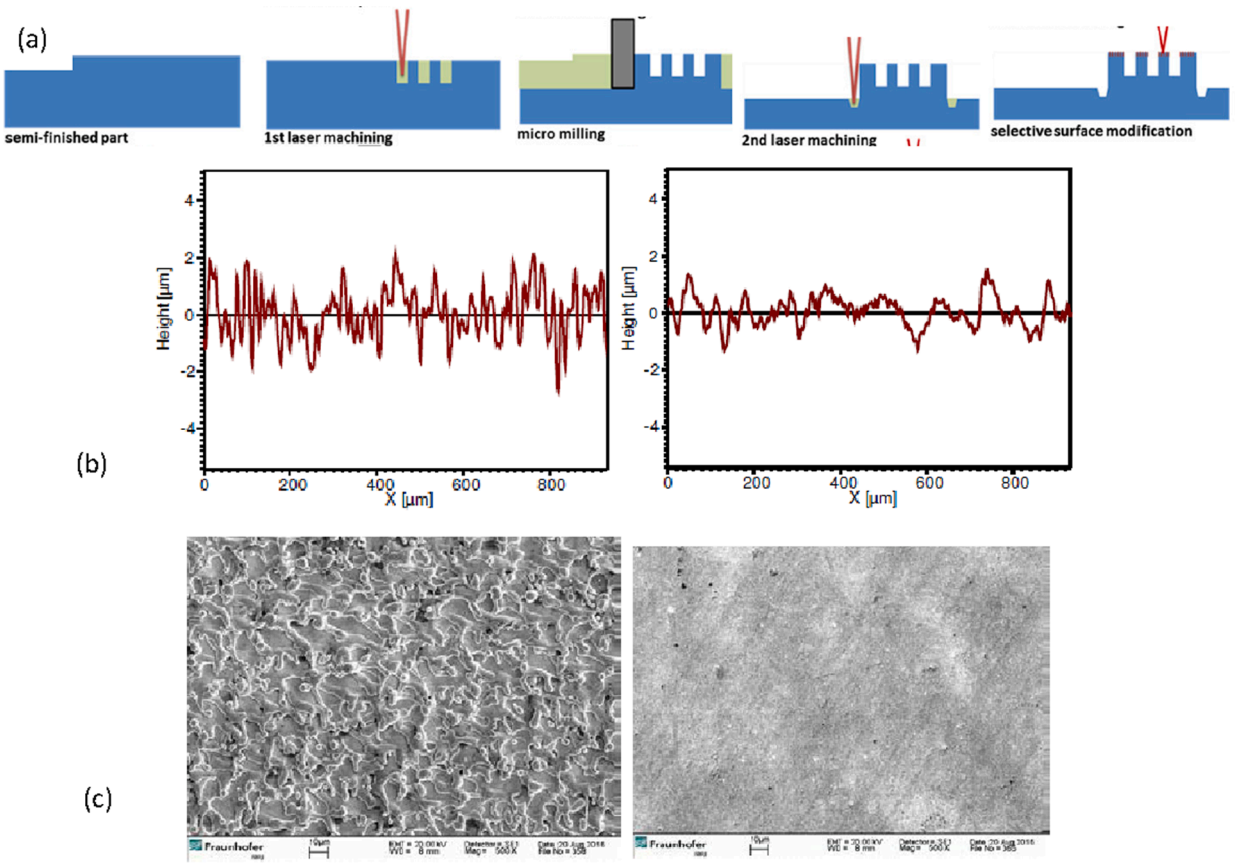

Fig. 51. (a) The sequential process of laser machining–milling with subsequent surface functionalization (b) Surface roughness of 5 µm after laser structuring and 2 µm after polishing and (c) structure comparison of the laser-structured areas and laser polished area [138]. [Reproduced by permission of the publisher. Permission to reuse must be obtained from the rights holder].

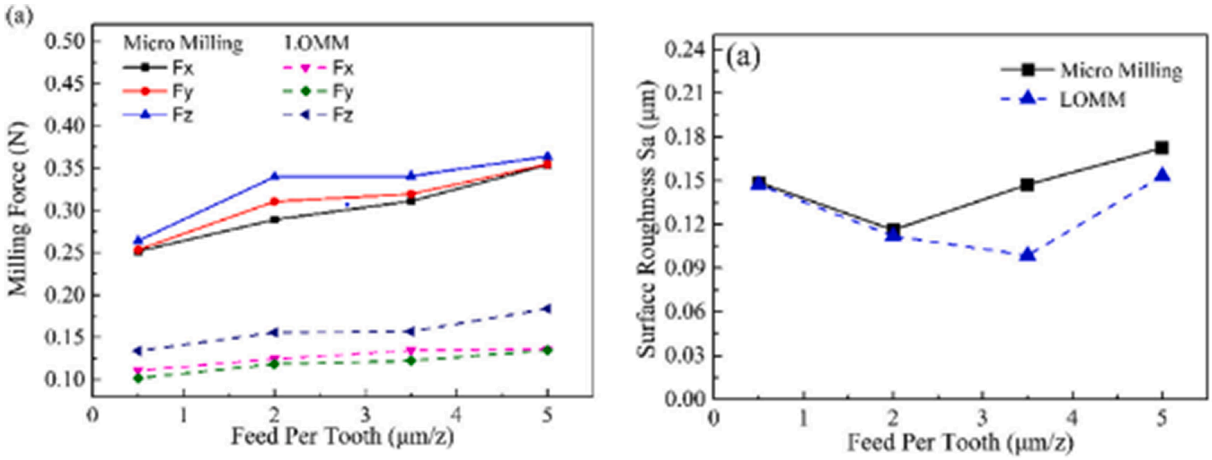

Fig. 52. Comparison of cutting force and surface roughness [109]. [Reproduced by permission of the publisher. Permission to reuse must be obtained from the rights holder].

Schubert et al. [137] combined micro-milling and LBM for fabricating complicated microstructures on hot embossing dies, which have applications in microfluidic systems. The milling cutter diameters of 0.1, 0.3 and 0.5 mm were used. The fabricated microstructures are shown in Fig. 50(b) and machining time for sequential and single milling processes with different tools are shown in Fig. 50(a).

Mould and dies are also fabricated by micro-milling laser structuring and laser polishing sequentially, as Grossa et al. [138] show. Sequential methods create an accurate geometrical dimension and are quick and more efficient machining of the component, as shown in Fig. 51 (a). Surface roughness in the microchannel obstructs flow in the system. After laser structuring, the roughness of 5 µm and polishing of 2 µm was achieved, as shown in Fig. 51(b). The corresponding surface structure is shown in Fig. 51(c), which shows polished laser surfaces are smoother in comparison to non-polished ones. Polishing reduces the surface peaks, and a better surface structure was achieved, as evident in Fig. 51 (c). The surface roughness creates interference of capillary filling for the microfluidic channel in the embossed part.

A new method of laser-induced oxygen assisted micro-milling was introduced by Xia et al. [109,156,172]. Oxygen is supplied during laser heating at 2 W of power by a pulsed fiber laser, forming an oxide layer on the surface and a sub-layer of oxide with lower hardness. So, the lower milling force and better surface finish of the micro-channel was achieved as shown in Fig. 52.

Kadivar et al. performed laser-assisted micro-milling of stainless steel. In the process, laser structure is formed on the surface, and the machining is performed with coolant assisted micro milling in achieving lower forces. The fundamental difference is here, instead of the heat energy of the laser beam, the surface has been structured so cracks axial cracks are developed. Results show lower nominal and tangential force with a structured surface. Also, the temperature developed due to tool machining was observed lower.[157].

Exploration of new laser-based micromachining process mechanics and feasibility studies for newly developed materials shows wide research and application scope of the process. Moreover, such kinds of investigations are very encouraging for newcomers who choose target materials and process mechanics to be explored. More such advancements in the process are needed so that the smallest aspects, application possibilities, and any process variants mat not remain untouched

6. Future scope

The primary research areas and researcher's contributions in laser-based hybrid micromachining are discussed in the previous sections. Due to the complexity of hybrid process mechanics, a lot of work is still required to be done. In the end, the process challenges with respective remedies and future scopes are presented.

- ***Industrial applications*:** Till now, laser-based hybrid micromachining processes have been confined to lab research only. In this decade, there is an expectation of converting lab research to industrial applications or in shapes of industry-ready products. An extensive study and necessary experimentation will be required to be done as per applications, so a cost-effective product with better quality can enter the market [139,140]. It can also collaborate with clinical research for different biocompatible structure fabrication. In MEMS, different geometries, lab on chips application on silicon and other materials can also be analyzed with these methods. Biocompatible and biodegradable stent manufacturing is an emerging application with the LHMMP process. Microfluidic structures, channels, and nozzles are applications for hybrid machining,
- ***System development*:** There is a need to develop systems capable of performing laser-based sequential and assisted machining on the same or different machine tools. Also, it is in demand to develop 3D complex geometrical products, which are still needed in real-life applications. For complex geometry, multi-axis systems need to be developed having five axes or more to integrate hybrid processes [141]. There should be provisions to combine conventional and non-conventional processes. So, the difficult geometries can easily be machined in any kind of material. If LBM assists EDM or ECM, it will limit the workpiece material range to only electric conductive material. So, there is a need to look for other options for electrically non-conductive materials [142]. If the sequential machining will be performed on the same machine, it helps avoid repositioning, which is a major drawback. If machining is performed on different stations, alignment of the processes will be critical. Misalignment can cause improper functioning of micro-devices. Some fixtures or devices will be needed, which can align reference planes of the workpiece for both the machines [143].
- **In situ *measurement and process monitoring*:** Precise components are required for miniature applications, so measurement in LHMMP is essential for maintaining the product's quality [69,144]. An in-situ metrology attachment needs to be developed and integrated into the micromachining system to measure and inspect the micro components produced during manufacturing. The data of measuring sensors will be directly fed into the machine controller for adaptive control of the processes [145,146]. If the laser machining is combined sequentially with conventional machining, a force and torque sensor is also needed to acquire feedback during micromachining and take further corrective actions. Geometric dimension and surface finish measurements will be needed in-between processes [147]. Noncontact measurement during the process or in-between processed through Microscope, Confocal sensor, or 3D profilometer can also be one option. Process monitoring includes temperature measurement, image processing, and tool wear measurement.
- ***Process development*:** In the future, researchers should actively look to combine laser with other processes like abrasive finishing, nano finishing process, RP systems, water jet machining, honing, ECH and others [148].

Sequential or assisted micromachining process + measurement + finishing = final product

Laser polishing is also emerging as one possibility, so necessary analysis with the same laser source or different can be done. A high degree of process control will be needed to combine assisted or sequential laser micromachining methods.

- ***Mechanism understanding*:** There is a requirement to develop new sequential and assisted processes and understand the mechanism of removal in these processes [149]. Understanding process physics and surface integrity, metallurgical characterization also needs to be done. Also, the theoretical mathematical model can help in Figuring out the mechanisms. The majority of laser-assisted processes in which laser energy is used either as a primary or secondary source for removal mechanism needs to be studied. Sequential process criticality and dependence on the removal mechanisms must be investigated in future studies [150].
- ***Cyber-Physical System development*:** In the upcoming era of manufacturing, machining systems are not only capable of machining, but also, they should be compatible with *i4.0*. A cyber-physical systems-based multiprocessor system needs to be developed to manufacture the actual 3D part without any end-user monitoring of the system. CPS-based applications need to be developed to verify the feasibility of proposed mechanisms, which calculates machining time, numbers of passes required to achieve targeted geometric dimensions, and roughness value based on the operator's input process parameters and roughness value [151].

7. Conclusion

The present article describes the overall review of the research and developments carried out in the Laser-based hybrid micromachining process and its application areas. This is envisaged as the technology for manufacturing highly complicated micro shapes with few microns of dimension on various engineering materials, especially for hard materials and biocompatible materials. In the upcoming decade, challenges will be to control the dimensional tolerances of micro parts for precision manufacturing of sub microns and nano-level with hybrid machining technology. After a comprehensive review of the previous research, challenges and future research scopes are also described.

Laser-based hybrid micromachining processes overcome the limitation of LBM and other conventional and non-conventional processes. Products with better surface integrity, better geometric tolerance, high precision, higher MRR, low-cost machining, higher productivity, lower machining time can be achieved by laser-based sequential and assisted machining. If LBM is combined with EDM, ECM, or conventional machining, lower tool wear has been achieved. Past studies show assisted and sequential LBM performance in the research area for micromanufacturing. However, complex 3D geometry creation will focus in the next decade on assisted and sequential machining. Laser

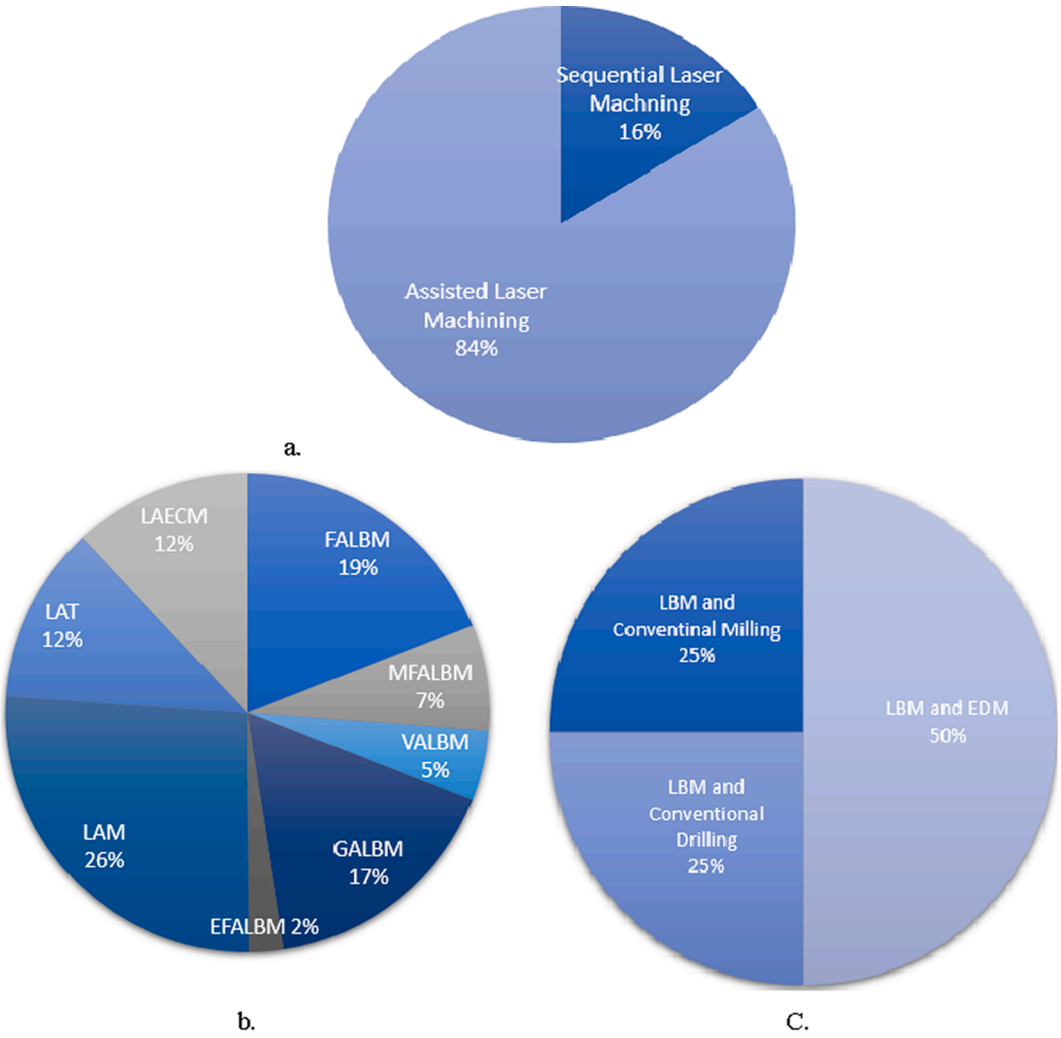

Fig. 53. (a) Research performed in laser-based hybrid machining processes. (b) Laser-assisted machining (c) Sequential laser machining process. [**VALBM** Vibration assisted LBM; **MFALBM** Magnetic field-assisted LBM**; FALBM** Fluid assisted LBM; **EFALBM** Electric field-assisted LBM; **GALBM** Gas-assisted LBM; **LAM** Laser-Assisted Milling; **LAECM** Laser-Assisted ECM; **LAT** Laser-Assisted Turning].

machining is the dominant technique for faster machining. Laser and EDM combined gave significant results as per studies reported in previous sections.

LHMMP has primary literature (84%) in the laser-assisted machining process, as evident in Fig. 53(a). In assisted machining, Laser-assisted milling (26%) work is performed, which is a major contributor in previous studies. The process has been analyzed mathematically, and modelling of the process is carried out. Fluid assisted LBM (19%) having a significant portion of water-assisted LBM. There is a need to investigate different liquids and chemicals also. Moreover, 17% of research has been carried out in gas-assisted LBM, which is favourable for efficient machining with different materials. Vibration assisted (5%) and Electric field-assisted (2%) are relatively new areas that need to be investigated further for micromachining applications and performance improvements.

In sequential laser machining, 50% study were reported in LBM and EDM sequential machining. This is due to post-laser machining, EDM improves the machined part's surface characteristics as shown in Fig. 53 (c). Sequential LBM and conventional milling (25%) is required to be investigated for 3D geometries and complex shapes. LAECM (12%) for improvement in ECM process.

Moreover, literature mostly belongs to process mechanism understanding, and there are no commercial applications in this area. Research is limited to two processes only, either in sequentially or assisted manner. In the future, if required, we need to look at more than two processes simultaneously or sequentially. There is a need to study process material interaction among different hybrid machining methods and develop a new approach. It is now concluded that LHMMP is quite novel and adaptable, which can deliver free form surfaces. Besides incorporating the LHMMP method, other hybrid machining methods can be considered and combined, which can be considered another intriguing subject as it would overcome various shortcomings confronted until now with the machining processes [152].

Declaration of Competing Interest

The authors declare that they have no known competing financial interests or personal relationships that could have appeared to influence the work reported in this paper.

Acknowledgement

The authors, would like to acknowledge the financial support under the Technology Development program from the Department of Science and Technology, Govt of India, to conduct research.

References

[1] P.C. Pandey, H.S. Shan, Modern machining processes, Tata McGraw-Hill Publishing Company Ltd, New Delhi, India, 1997.
[2] Micro-Manufacturing Technologies and Their Applications A Theoretical and Practical Guide Editors Irene Fassi David Shipley.
[3] N. Zhang, J. Liu, H. Zhang, N.J. Kent, D. Diamond, M.D. Gilchrist, 3D. Micromachines 2019;10. Doi: 10.3390/mi10090595.
[4] S.P. Leo, J. Jerald, S. Kumanan, Manufacturing Application of Micromachining for Automobile Components (2012) 4–8.
[5] J. Gong, Q. Chen, W. Fei, S. Seal, Micromachined nanocrystalline SnO2 chemical gas sensors for electronic nose, Sens. Actuators, B Chem. 102 (2004) 117–125, https://doi.org/10.1016/j.snb.2004.02.055.
[6] T. Masuzawa, H.K. Tönshoff, Three-dimensional micromachining by machine tools, CIRP Ann. 46 (1997) 621–628, https://doi.org/10.1016/S0007-8506(07)60882-8.
[7] Micromanufacturing: An Introduction By V.K. Jain, Ajay Sidpara, M. Ravisankar, and Manas Das.
[8] P. Abgrall, A.M. Gué, Lab-on-chip technologies: Making a microfluidic network and coupling it into a complete microsystem - A review, J. Micromech. Microeng. 17 (2007), https://doi.org/10.1088/0960-1317/17/5/R01.
[9] H.N. Hansen, R.J. Hocken, G. Tosello, Replication of micro and nano surface geometries, CIRP Ann. 60 (2011) 695–714, https://doi.org/10.1016/J.CIRP.2011.05.008.
[10] A.E. Guber, M. Heckele, D. Herrmann, A. Muslija, V. Saile, L. Eichhorn, et al., Microfluidic lab-on-a-chip systems based on polymers - fabrication and application, Chem. Eng. J. 101 (2004) 447–453, https://doi.org/10.1016/j.cej.2004.01.016.
[11] T.O. Samir Mekid, Azfar Khalid, Common physical problems in micromachining, 6th CIRP Int. Conf. Intell. Comput. Manuf. Eng. - CIRP ICME '08, Ischia (Naples), Italy. (2008).
[12] M. Takacs, Micro Machining and Hard Cutting – Challenges of Modern Manufacturing Technology, (2015) 84177.
[13] E. Uhlmann, B. Mullany, D. Biermann, K.P. Rajurkar, T. Hausotte, E. Brinksmeier, Process chains for high-precision components with micro-scale features, CIRP Ann.. – Manuf. Technol. 65 (2016) 549–572, https://doi.org/10.1016/j.cirp.2016.05.001.
[14] Z. Zhang, J. Yan, T. Kuriyagawa, Manufacturing technologies toward extreme precision, Int J Extrem Manuf 1 (2019), 022001, https://doi.org/10.1088/2631-7990/ab1ff1.
[15] L. Micheli, N. Sarmah, X. Luo, K.S. Reddy, T.K. Mallick, Opportunities and challenges in micro- and nano-technologies for concentrating photovoltaic cooling: A review, Renew. Sustain. Energy Rev. 20 (2013) 595–610, https://doi.org/10.1016/J.RSER.2012.11.051.
[16] Hybrid Machining Theory, Methods, and Case Studies 2018, Pages 21-41 Overview of Hybrid Machining Processes.
[17] I. Science, State of the Art of Micromachining, 49 (2000).
[18] A.B.M.A. Asad, T. Masaki, M. Rahman, H.S. Lim, Y.S. Wong, Tool-based micromachining, J. Mater. Process. Technol. 192–193 (2007) 204–211, https://doi.org/10.1016/J.JMATPROTEC.2007.04.038.
[19] Ã NMA, D.G. Solomon, F. Bahari, A review on current research trends in electrical discharge machining 2007;47:1214–28. Doi: 10.1016/j.ijmachtools.2006.08.026.
[20] A. Spieser, A. Ivanov, Recent developments and research challenges in electrochemical micromachining (μECM) 2013:563–81, Doi: 10.1007/s00170-013-5024-8.
[21] L. Alting, F. Kimura, H.N. Hansen, G. Bissacco, Micro engineering, CIRP Ann. 52 (2003) 635–657, https://doi.org/10.1016/S0007-8506(07)60208-X.
[22] H. Huang, H. Zhang, L. Zhou, H.Y. Zheng, Ultrasonic vibration assisted electro-discharge machining of microholes in Nitinol, J. Micromech. Microeng. 13 (2003) 693–700, https://doi.org/10.1088/0960-1317/13/5/322.
[23] M. Rahman, A.B.M.A. Asad, T. Masaki, T. Saleh, Y.S. Wong, A.S. Kumar, International Journal of Machine Tools & Manufacture A multiprocess machine tool for compound micromachining, Int. J. Mach. Tools Manuf. 50 (2010) 344–356, https://doi.org/10.1016/j.ijmachtools.2009.10.007.
[24] K. Singh, S.K. Maurya, S. Kumar, A review on introduction to hybrid machining process 1-3, (2018) 22–26.
[25] M.C. Gower, Industrial applications of pulsed laser micromachining, Conf Lasers Electro-Optics Eur - Tech Dig 7 (1998) 247, https://doi.org/10.1109/cleoe.1998.719333.
[26] E. Williams, E.B. Brousseau, Simulation and experimental study of nanosecond laser micromachining of commercially pure titanium, J. Micro Nano-Manuf. 4 (2015), 011004, https://doi.org/10.1115/1.4031892.
[27] V. Zdeněk, H. Milan, M. Jiří, 3D model of laser treatment by a moving heat source with general distribution of energy in the beam, Appl. Opt. 55 (2016) D140, https://doi.org/10.1364/ao.55.00d140.
[28] Q. Zhang, C. Wang, Y. Liu, L. Zhang, G. Cheng, Picosecond laser machining of deep holes in silicon infiltrated silicon carbide ceramics, J. Wuhan Univ. Technol. Sci. Ed. 30 (2015) 437–441, https://doi.org/10.1007/s11595-015-1167-9.
[29] Y. Zhang, D. Zhang, J. Wu, Z. He, X. Deng, A thermal model for nanosecond pulsed laser ablation of aluminum, AIP Adv. 7 (2017), https://doi.org/10.1063/1.4995972.
[30] K. Voisey, T. Clyne, Laser drilling of cooling holes through plasma sprayed thermal barrier coatings, Surf. Coatings Technol. 176 (2004) 296–306, https://doi.org/10.1016/S0257-8972(03)00748-5.
[31] R. Biswas, A.S. Kuar, S.K. Biswas, S. Mitra, Artificial neural network modelling of Nd:YAG laser microdrilling on titanium nitride-alumina composite, Proc. Inst. Mech. Eng. Part B J. Eng. Manuf. 224 (2010) 473–482. Doi: 10.1243/09544054JEM1576.
[32] S. Panda, D. Mishra, B.B. Biswal, Determination of optimum parameters with multi-performance characteristics in laser drilling-A grey relational analysis approach, Int. J. Adv. Manuf. Technol. 54 (2011) 957–967, https://doi.org/10.1007/s00170-010-2985-8.
[33] A.S. Kuar, B. Doloi, B. Bhattacharyya, Modelling and analysis of pulsed Nd:YAG laser machining characteristics during micro-drilling of zirconia (ZrO2), Int. J. Mach. Tools Manuf. 46 (2006) 1301–1310, https://doi.org/10.1016/J.IJMACHTOOLS.2005.10.016.
[34] C.A. McNally, J. Folkes, I.R. Pashby, Laser drilling of cooling holes in aeroengines: state of the art and future challenges, Doi: 10.1179/026708304225017391.
[35] D. Dhupal, B. Doloi, B. Bhattacharyya, Modeling and optimization on Nd:YAG laser turned micro-grooving of cylindrical ceramic material, Opt. Lasers Eng. 47 (2009) 917–925, https://doi.org/10.1016/j.optlaseng.2009.03.016.
[36] N. Muhammad, D. Whitehead, A. Boor, W. Oppenlander, Z. Liu, L. Li, Picosecond laser micromachining of nitinol and platinum-iridium alloy for coronary stent applications, Appl. Phys. A Mater. Sci. Process. 106 (2012) 607–617, https://doi.org/10.1007/s00339-011-6609-4.
[37] B. Stępak, A.J. Antończak, M. Bartkowiak-Jowsa, J. Filipiak, C. Pezowicz, K. M. Abramski, Fabrication of a polymer-based biodegradable stent using a CO2 laser, Arch. Civ. Mech. Eng. 14 (2014) 317–326, https://doi.org/10.1016/J.ACME.2013.08.005.
[38] A.G. Demir, B. Previtali, B. Çetin, Laser micro-milling for the fabrication of a microfluidic device mold, 2015.
[39] Investigation of the piercing process in laser cutting of stainless steel J. Laser Appl., 29, 022201 (2017); Doi: 10.2351/1.4983260.
[40] Parameter optimisation in laser cutting of aluminium alloy sheet July 2012 Int. J. Mech. Manuf. Syst. 5(3/4):179 – 188 DOI: 10.1504/IJMMS.2012.048227.
[41] Y. Wu, A.H. Wang, R.R. Zheng, H.Q. Tang, X.Y. Qi, B. Ye, Laser-drilled micro-hole arrays on polyurethane synthetic leather for improvement of water vapor permeability, Appl. Surf. Sci. 305 (2014) 1–8, https://doi.org/10.1016/J.APSUSC.2014.02.069.
[42] Copper vapor laser drilling of copper, iron, and titanium foils In atmospheric pressure air and argon J. Lash JS, Gilgenbach RM. reset 1993;64:3308–13.
[43] C.A. Biffi, N. Lecis, B. Previtali, M. Vedani, G.M. Vimercati, Fiber laser microdrilling of titanium and its effect on material microstructure, Int. J. Adv. Manuf. Technol. 54 (2011) 149–160, https://doi.org/10.1007/s00170-010-2918-6.
[44] S.T. Hendow, R. Romero, S.a. Shakir, P.T. Guerreiro, Percussion drilling of metals using bursts of nanosecond pulses, Opt. Express 19 (2011) 10221–10231, https://doi.org/10.1364/OE.19.010221.
[45] A. Weck, T.H.R. Crawford, D.S. Wilkinson, H.K. Haugen, J.S. Preston, Laser drilling of high aspect ratio holes in copper with femtosecond, picosecond and nanosecond pulses, Appl. Phys. A Mater. Sci. Process. 90 (2008) 537–543, https://doi.org/10.1007/s00339-007-4300-6.
[46] S. Lazare, J. Lopez, F. Weisbuch, High-aspect-ratio microdrilling in polymeric materials with intense KrF laser radiation, Appl. Phys. A Mater. Sci. Process. 69 (1999) 2–7, https://doi.org/10.1007/s003399900218.
[47] G. Kibria, B. Doloi, B. Bhattacharyya, Experimental investigation and multi-objective optimization of Nd:YAG laser micro-turning process of alumina ceramic using orthogonal array and grey relational analysis, Opt. Laser Technol. 48 (2013) 16–27, https://doi.org/10.1016/j.optlastec.2012.09.036.
[48] I.E. Saklakoglu, S. Kasman, Investigation of micro-milling process parameters for surface roughness and milling depth, Int. J. Adv. Manuf. Technol. 54 (2011) 567–578, https://doi.org/10.1007/s00170-010-2953-3.
[49] C.K. Desai, A. Shaikh, Prediction of depth of cut for single-pass laser micro-milling process using semi-analytical, ANN and GP approaches, Int. J. Adv. Manuf. Technol. 60 (2012) 865–882, https://doi.org/10.1007/s00170-011-3677-8.
[50] W. Zhou, W. Deng, L. Lu, J. Zhang, L. Qin, S. Ma, et al., Laser micro-milling of microchannel on copper sheet as catalyst support used in microreactor for hydrogen production, Int. J. Hydrogen Energy 39 (2014) 4884–4894, https://doi.org/10.1016/j.ijhydene.2014.01.041.
[51] L. Li, D.K.Y. Low, M. Ghoreshi, J.R. Crookall, Hole taper characterisation and control in laser percussion drilling, CIRP Ann. 51 (2002) 153–156, https://doi.org/10.1016/S0007-8506(07)61488-7.
[52] J. Dutta Majumdar, I. Manna, Laser material processing, Int. Mater. Rev. 56 (2011) 341–388, https://doi.org/10.1179/1743280411Y.0000000003.
[53] Y.J. Chang, C.L. Kuo, N.Y. Wang, Magnetic assisted laser micromachining for highly reflective metals, J. Laser Micro Nanoeng. 7 (2012) 254–259, https://doi.org/10.2961/jlmn.2012.03.0004.
[54] S. Chatterjee, S.S. Mahapatra, V. Bharadwaj, A. Choubey, B.N. Upadhyay, K. S. Bindra, Drilling of micro-holes on titanium alloy using pulsed Nd:YAG laser: Parametric appraisal and prediction of performance characteristics, Proc. Inst. Mech. Eng. Part B J. Eng. Manuf. 233 (2019) 1872–1889, https://doi.org/10.1177/0954405418805604.
[55] H. Dong, Y. Huang, Y. Rong, C. Chen, W. Li, Z. Gao, 532 nm Nanosecond laser cutting solar float glass: Surface quality evaluation with different laser spot positions in field lens, Optik 223 (September) (2020), 165620, https://doi.org/10.1016/j.ijleo.2020.165620.
[56] P.G. Benardos, G.-C. Vosniakos, Predicting surface roughness in machining: a review, Int. J. Mach. Tools Manuf. 43 (2003) 833–844, https://doi.org/10.1016/S0890-6955(03)00059-2.

[57] N. Ahmed, S. Darwish, A.M. Alahmari, Experimental Investigation of Dimensional Variation in Laser- machined Micro-channels produced in Titanium Alloy 2016; 11:210–26. Doi: 10.2961/jlmn.2016.02.0012.

[58] W.T. Chien, S.C. Hou, Investigating the recast layer formed during the laser trepan drilling of Inconel 718 using the Taguchi method, Int. J. Adv. Manuf. Technol. 33 (2007) 308–316, https://doi.org/10.1007/s00170-006-0454-1.

[59] A.F.M. Arif, B.S. Yilbas, Thermal stress developed during the laser cutting process : consideration of different materials 2008:698–704. Doi: 10.1007/s00170-007-1020-1.

[60] W. Choi, H.Y. Kim, J.W. Jeon, W.S. Chang, S.H. Cho, Vibration-assisted femtosecond laser drilling with controllable taper angles for AMOLED fine metal mask fabrication, Materials (Basel) 10 (2017), https://doi.org/10.3390/ma10020212.

[61] L. Romoli, R. Vallini, Experimental study on the development of a micro-drilling cycle using ultrashort laser pulses, Opt. Lasers Eng. 78 (2016) 121–131, https://doi.org/10.1016/j.optlaseng.2015.10.010.

[62] L. Zhang, H. Tong, Y. Li, Precision machining of micro tool electrodes in micro EDM for drilling array micro holes, Precis. Eng. 39 (2015) 100–106, https://doi.org/10.1016/j.precisioneng.2014.07.010.

[63] M.P. Jahan, Y.S. Wong, M. Rahman, A study on the quality micro-hole machining of tungsten carbide by micro-EDM process using transistor and RC-type pulse generator, J. Mater. Process. Technol. 209 (2009) 1706–1716, https://doi.org/10.1016/J.JMATPROTEC.2008.04.029.

[64] I. Tansel, T. Arkan, W. Bao, N. Mahendrakar, B. Shisler, D. Smith, et al., Tool wear estimation in micromachining: Part I: tool usage–cutting force relationship, Int. J. Mach. Tools Manuf. 40 (2000) 599–608, https://doi.org/10.1016/S0890-6955(99)00073-5.

[65] Y. Qin, A. Brockett, Y. Ma, A. Razali, J. Zhao, C. Harrison, et al., Micro-manufacturing: Research, technology outcomes and development issues, Int. J. Adv. Manuf. Technol. 47 (2010) 821–837, https://doi.org/10.1007/s00170-009-2411-2.

[66] I.G. Reichenbach, M. Bohley, F.J.P. Sousa, J.C. Aurich, Micromachining of PMMA—manufacturing of burr-free structures with single-edge ultra-small micro end mills, Int. J. Adv. Manuf. Technol. 96 (2018) 3665–3677, https://doi.org/10.1007/s00170-018-1821-4.

[67] A. Honegger, S.G. Kapoor, R.E. DeVor, A hybrid methodology for kinematic calibration of micro/meso-scale machine tools (mMTs), J. Manuf. Sci. Eng. Trans. ASME 128 (2006) 513–522, https://doi.org/10.1115/1.2162910.

[68] K. Vacharanukul, S. Mekid, In-process dimensional inspection sensors, Measurement 38 (2005) 204–218, https://doi.org/10.1016/J.MEASUREMENT.2005.07.009.

[69] S. Jha, A. Kumar, F. Iqbal, A.K. Sahu, In situ geometric measurement of microchannels on EN31 steel by laser micromachining using confocal sensor, Int. J. Precis. Technol. 8 (2019) 1, https://doi.org/10.1504/ijptech.2019.10021796.

[70] A.K.M. De Silva, P.T. Pajak, J.A. McGeough, D.K. Harrison, Thermal effects in laser assisted jet electrochemical machining, CIRP Ann.. – Manuf. Technol. 60 (2011) 243–246, https://doi.org/10.1016/j.cirp.2011.03.132.

[71] S.Z. Chavoshi, S. Goel, P. Morantz, Current trends and future of sequential micromachining processes on a single machine tool, Mater. Des. 127 (2017) 37–53, https://doi.org/10.1016/j.matdes.2017.04.057.

[72] K. Gupta, N.K. Jain, R.F. Laubscher, Hybrid machining processes perspectives on machining and finishing, 2016, Doi: 10.1007/978-3-319-25922-2.

[73] B. Lauwers, F. Klocke, A. Klink, A.E. Tekkaya, R. Neugebauer, D. Mcintosh, Hybrid processes in manufacturing, CIRP Ann. 63 (2014) 561–583, https://doi.org/10.1016/J.CIRP.2014.05.003.

[74] M.M. Okasha, P.T. Mativenga, N. Driver, L. Li, CIRP annals - manufacturing technology sequential laser and mechanical micro-drilling of Ni superalloy for aerospace application, CIRP Ann.. – Manuf. Technol. 59 (2010) 199–202, https://doi.org/10.1016/j.cirp.2010.03.011.

[75] R. Teti, K. Jemielniak, G. O'Donnell, D. Dornfeld, Advanced monitoring of machining operations, CIRP Ann. 59 (2010) 717–739, https://doi.org/10.1016/J.CIRP.2010.05.010.

[76] H.Y. Zheng, H. Huang, Ultrasonic vibration-assisted femtosecond laser machining of microholes, J. Micromech. Microeng. 17 (2007), https://doi.org/10.1088/0960-1317/17/8/N03.

[77] H.Y. Zheng, H. Huang, Ultrasonic vibration-assisted femtosecond laser machining of microholes, J. Micromech. Microeng. 17 (2007), https://doi.org/10.1088/0960-1317/17/8/N03.

[78] S.H. Alavi, S.P. Harimkar, Ultrasonic vibration-assisted continuous wave laser surface drilling of materials, Manuf. Lett. 4 (2015) 1–5, https://doi.org/10.1016/j.mfglet.2015.01.002.

[79] J.K. Park, J.W. Yoon, S.H. Cho, Vibration assisted femtosecond laser machining on metal, Opt. Lasers Eng. 50 (2012) 833–837, https://doi.org/10.1016/j.optlaseng.2012.01.017.

[80] C.C. Ho, C.M. Chiu, Y.J. Chang, J.C. Hsu, C.L. Kuo, Magnetic-field-assisted laser percussion drilling, Int. J. Adv. Manuf. Technol. 73 (2014) 329–340, https://doi.org/10.1007/s00170-014-5815-6.

[81] I. Saxena, S. Wolff, J. Cao, Unidirectional magnetic field assisted laser induced plasma micromachining, Manuf. Lett. 3 (2015) 1–4, https://doi.org/10.1016/j.mfglet.2014.09.001.

[82] C.-C. Ho, G.-R. Tseng, Y.-J. Chang, J.-C. Hsu, C.-L. Kuo, External electric field-assisted laser percussion drilling for highly reflective metals, Adv. Mech. Eng. 5 (2013), 156707, https://doi.org/10.1155/2013/156707.

[83] H.Y. Zheng, Z.W. Jiang, Femtosecond laser micromachining of silicon with an external electric field, J. Micromech. Microeng. 20 (2010), https://doi.org/10.1088/0960-1317/20/1/017001.

[84] A. Samanta, M. Teli, R. Singh, Experimental characterization and finite element modeling of the residual stresses in laser-assisted mechanical micromachining of Inconel 625, Proc. Inst. Mech. Eng. Part B J. Eng. Manuf. 231 (2017) 1735–1751, https://doi.org/10.1177/0954405415612677.

[85] X.W. Cao, Q.D. Chen, H. Fan, L. Zhang, S. Juodkazis, H.B. Sun, Liquid-assisted femtosecond laser precision-machining of silica, Nanomaterials 8 (2018) 1–8, https://doi.org/10.3390/nano8050287.

[86] A.M. Alahmari, N. Ahmed, S. Darwish, Laser beam micromachining under water immersion, Int. J. Adv. Manuf. Technol. 83 (2016) 1671–1681, https://doi.org/10.1007/s00170-015-7699-5.

[87] V. Mistry, S. James, Finite element analysis and simulation of liquid-assisted laser beam machining process, Int. J. Adv. Manuf. Technol. 94 (2018) 2325–2331, https://doi.org/10.1007/s00170-017-1009-3.

[88] R.R. Behera, M.R. Sankar, J. Swaminathan, I. Kumar, A.K. Sharma, A. Khare, Experimental investigation of underwater laser beam micromachining (UW-LBμM) on 304 stainless steel, Int. J. Adv. Manuf. Technol. 85 (2016) 1969–1982, https://doi.org/10.1007/s00170-016-8635-z.

[89] T. Wuttisarn, V. Tangwarodomnukun, C. Dumkum, Laser micro-milling under a thin and flowing water layer: A new concept of liquid-assisted laser machining process, Proc. Inst. Mech. Eng. Part B J. Eng. Manuf. 230 (2016) 376–380, https://doi.org/10.1177/0954405415580542.

[90] L.M. Wee, E.Y.K. Ng, A.H. Prathama, H. Zheng, Micromachining of silicon wafer in air and under water, Opt. Laser Technol. 43 (2011) 62–71, https://doi.org/10.1016/j.optlastec.2010.05.005.

[91] C.K. Chung, H.C. Chang, T.R. Shih, S.L. Lin, E.J. Hsiao, Y.S. Chen, et al., Water-assisted CO2laser ablated glass and modified thermal bonding for capillary-driven bio-fluidic application, Biomed. Microdevices 12 (2010) 107–114, https://doi.org/10.1007/s10544-009-9365-x.

[92] R. An, Y. Li, Y. Dou, D. Liu, H. Yang, Q. Gong, Water-assisted drilling of microfluidic chambers inside silica glass with femtosecond laser pulses, Appl. Phys. A Mater. Sci. Process. 83 (2006) 27–29, https://doi.org/10.1007/s00339-005-3456-1.

[93] R. An, M.D. Hoffman, M.A. Donoghue, A.J. Hunt, S.C. Jacobson, Water-assisted femtosecond laser machining of electrospray nozzles on glass microfluidic devices, Opt. Express 16 (2008) 15206–15211, https://doi.org/10.1364/oe.16.015206.

[94] C. Barnes, P. Shrotriya, P. Molian, Water-assisted laser thermal shock machining of alumina, Int. J. Mach. Tools Manuf. 47 (2007) 1864–1874, https://doi.org/10.1016/j.ijmachtools.2007.04.003.

[95] A. Riveiro, F. Quintero, F. Lusquiños, R. Comesaña, J. Pou, Parametric investigation of CO2laser cutting of 2024–T3 alloy, J. Mater. Process. Technol. 210 (2010) 1138–1152, https://doi.org/10.1016/j.jmatprotec.2010.02.024.

[96] A. Riveiro, F. Quintero, M. Boutinguiza, J. del Val, R. Comesaña, F. Lusquiños, et al., Laser cutting: A review on the influence of assist gas, Materials (Basel) 12 (2019), https://doi.org/10.3390/ma12010157.

[97] O.S. Bursi, M. D'Incau, G. Zanon, S. Raso, P. Scardi, Laser and mechanical cutting effects on the cut-edge properties of steel S355N, J. Constr. Steel Res. 133 (2017) 181–191, https://doi.org/10.1016/J.JCSR.2017.02.012.

[98] C.Y. Jiang, W.S. Lau, T.M. Yue, L. Chiang, On the maximum depth and profile of cut in pulsed Nd: YAG laser machining, CIRP Ann. 42 (1993) 223–226, https://doi.org/10.1016/S0007-8506(07)62430-5.

[99] J. Powell, D. Petring, R.V. Kumar, S.O. Al-Mashikhi, A.F.H. Kaplan, K.T. Voisey, Laser-oxygen cutting of mild steel: The thermodynamics of the oxidation reaction, J. Phys. D Appl. Phys. 42 (2009), https://doi.org/10.1088/0022-3727/42/1/015504.

[100] J. Mikoláš, P. Šugár, Micromachining of austenitic steel by pulsed Nd: Yag laser, Technol. Eng. 9 (2014) 21–23, https://doi.org/10.2478/teen-2012-0006.

[101] M.J. Jackson, G.M. Robinson, Micromachining electrical grade steel using pulsed Nd-YAG lasers, J. Achiev. Mater. Manuf. Eng. 20 (2007) 451–454.

[102] L. Shanjin, W. Yang, An investigation of pulsed laser cutting of titanium alloy sheet, Opt. Lasers Eng. 44 (2006) 1067–1077, https://doi.org/10.1016/J.OPTLASENG.2005.09.003.

[103] A. Riveiro, F. Quintero, F. Lusquiños, R. Comesaña, J. Pou, Effects of processing parameters on laser cutting of aluminium–copper alloys using off-axial supersonic nozzles, Appl. Surf. Sci. 257 (2011) 5393–5397, https://doi.org/10.1016/J.APSUSC.2010.11.061.

[104] A. Riveiro, F. Quintero, F. Lusquiños, R. Comesaña, J. Del Val, J. Pou, The role of the assist gas nature in laser cutting of aluminum alloys, Phys. Procedia 12 (2011) 548–554, https://doi.org/10.1016/j.phpro.2011.03.069.

[105] D.J. Hwang, T.Y. Choi, C.P. Grigoropoulos, Liquid-assisted femtosecond laser drilling of straight and three-dimensional microchannels in glass, Appl. Phys. A Mater. Sci. Process. 79 (2004) 605–612, https://doi.org/10.1007/s00339-004-2547-8.

[106] P. Dumitrescu, P. Koshy, J. Stenekes, M.A. Elbestawi, High-power diode laser assisted hard turning of AISI D2 tool steel, Int. J. Mach. Tools Manuf. 46 (2006) 2009–2016, https://doi.org/10.1016/J.IJMACHTOOLS.2006.01.005.

[107] O. Abdulghani, M. Sobih, A. Youssef, A.-M. El-Batahgy, Modeling and simulation of laser assisted turning of hard steels, Model Numer. Simul. Mater. Sci. 03 (2013) 106–113, https://doi.org/10.4236/mnsms.2013.34014.

[108] M.S. Brown, C.B. Arnold, Laser Precision Microfabrication 135 (2010) 91–120, https://doi.org/10.1007/978-3-642-10523-4.

[109] J.W. Ahn, W.S. Woo, C.M. Lee, A study on the energy efficiency of specific cutting energy in laser-assisted machining, Appl. Therm. Eng. 94 (2016) 748–753, https://doi.org/10.1016/J.APPLTHERMALENG.2015.10.129.

[110] Y. Wang, LJ, N.J. Wang, An investigation of laser-assisted machining of Al 2 O 3 particle reinforced aluminum matrix composite, J. Mater. Process Technol. 2002; 129:268–72.
[111] A. Panjehpour, M.R. Soleymani Yazdi, R. Shoja-Razavi, An experimental investigation of pulsed laser-assisted machining of AISI 52100 steel, Opt. Laser Technol. 63 (2014) 137–143, https://doi.org/10.1016/j.optlastec.2014.03.018.
[112] H. Mohammadi, D. Ravindra, S.K. Kode, J.A. Patten, Experimental work on micro laser-assisted diamond turning of silicon (111), J. Manuf. Process. 19 (2015) 125–128, https://doi.org/10.1016/j.jmapro.2015.06.007.
[113] D. Ravindra, M.K. Ghantasala, J. Patten, Ductile mode material removal and high-pressure phase transformation in silicon during micro-laser assisted machining, Precis. Eng. 36 (2012) 364–367, https://doi.org/10.1016/j.precisioneng.2011.12.003.
[114] K. Venkatesan, R. Ramanujam, P. Kuppan, Analysis of cutting forces and temperature in laser assisted machining of inconel 718 using taguchi method, Procedia Eng. 97 (2014) 1637–1646, https://doi.org/10.1016/j.proeng.2014.12.314.
[115] Y. Ayed, G. Germain, Salem W. Ben, H. Hamdi, Experimental and numerical study of laser-assisted machining of Ti6Al4V titanium alloy, Finite Elem. Anal. Des. 92 (2014) 72–79, https://doi.org/10.1016/j.finel.2014.08.006.
[116] G. Singh, M. Teli, A. Samanta, R. Singh, Finite element modeling of laser-assisted machining of AISI D2 tool steel, Mater. Manuf. Process. 28 (2013) 443–448, https://doi.org/10.1080/10426914.2012.700160.
[117] E. Kuram, B. Ozcelik, Multi-objective optimization using Taguchi based grey relational analysis for micro-milling of Al 7075 material with ball nose end mill, Meas. J. Int. Meas. Confed. 46 (2013) 1849–1864, https://doi.org/10.1016/j.measurement.2013.02.002.
[118] J.A. Shelton, Y.C. Shin, Comparative evaluation of laser-assisted micro-milling for AISI 316, AISI 422, TI-6AL-4V and Inconel 718 in a side-cutting conFigureuration, J. Micromech. Microeng. 20 (2010) 12, https://doi.org/10.1088/0960-1317/20/7/075012.
[119] C. Liu, Y. Shi, Modelling and simulation of laser assisted milling process of titanium alloy, Procedia CIRP 24 (2014) 134–139, https://doi.org/10.1016/j.procir.2014.08.004.
[120] H. Ding, N. Shen, Y.C. Shin, Thermal and mechanical modeling analysis of laser-assisted micro-milling of difficult-to-machine alloys, J. Mater. Process. Technol. 212 (2012) 601–613, https://doi.org/10.1016/j.jmatprotec.2011.07.016.
[121] S. Melkote, M. Kumar, F. Hashimoto, G. Lahoti, Laser assisted micro-milling of hard-to-machine materials, CIRP Ann. – Manuf. Technol. 58 (2009) 45–48, https://doi.org/10.1016/j.cirp.2009.03.053.
[122] K. Venkatesan, R. Ramanujam, Statistical approach for optimization of influencing parameters in laser assisted machining (LAM) of inconel alloy, Meas. J. Int. Meas. Confed. 89 (2016) 97–108, https://doi.org/10.1016/j.measurement.2016.04.021.
[123] R. Singh, S.N. Melkote, Experimental characterization of Laser-Assisted Mechanical Micromachining (LAMM) process, Am. Soc. Mech. Eng. Manuf. Eng. Div. MED 16–2 (2005) 1–8, https://doi.org/10.1115/IMECE2005-81350.
[124] J. Yang, S. Sun, M. Brandt, W. Yan, Experimental investigation and 3D finite element prediction of the heat affected zone during laser assisted machining of Ti6Al4V alloy, J. Mater. Process. Technol. 210 (2010) 2215–2222, https://doi.org/10.1016/j.jmatprotec.2010.08.007.
[125] R. Singh, M.J. Alberts, S.N. Melkote, Characterization and prediction of the heat-affected zone in a laser-assisted mechanical micromachining process, Int. J. Mach. Tools Manuf. 48 (2008) 994–1004, https://doi.org/10.1016/j.ijmachtools.2008.01.004.
[126] F. Tagliaferri, G. Leopardi, U. Semmler, M. Kuhl, B. Palumbo, Study of the influences of laser parameters on laser assisted machining processes, Procedia CIRP 8 (2013) 170–175, https://doi.org/10.1016/J.PROCIR.2013.06.084.
[127] A. Bucciarelli, P.D. Kuila, S.N. Melkote, A. Fortunato, Micro-machinability of A-286 steel with and without laser assist, Procedia CIRP 46 (2016) 432–435, https://doi.org/10.1016/j.procir.2016.04.049.
[128] P.T. Pajak, A.K.M. De Silva, J.A. McGeough, D.K. Harrison, Modelling the aspects of precision and efficiency in laser-assisted jet electrochemical machining (LAJECM), J. Mater. Process. Technol. 149 (2004) 512–518, https://doi.org/10.1016/j.jmatprotec.2003.10.055.
[129] P.T. Pajak, A.K.M. Desilva, D.K. Harrison, J.A. Mcgeough, Precision and efficiency of laser assisted jet electrochemical machining 30 (2006) 288–298, https://doi.org/10.1016/j.precisioneng.2005.09.006.
[130] A.K.M. DeSilva, P.T. Pajak, D.K. Harrison, J.A. McGeough, Modelling and experimental investigation of laser assisted jet electrochemical machining, CIRP Ann. 53 (2004) 179–182, https://doi.org/10.1016/S0007-8506(07)60673-8.
[131] H. Zhang, J. Xu, J. Wang, Investigation of a novel hybrid process of laser drilling assisted with jet electrochemical machining, Opt. Lasers Eng. 47 (2009) 1242–1249, https://doi.org/10.1016/j.optlaseng.2009.05.009.
[132] L. Li, C. Diver, J. Atkinson, R. Giedl-Wagner, H.J. Helml, Sequential laser and EDM micro-drilling for next generation fuel injection nozzle manufacture, CIRP Ann. – Manuf. Technol. 55 (2006) 179–182, https://doi.org/10.1016/S0007-8506(07)60393-X.
[133] M. Afiq Rashid, M. Rahman, Kumar A. Senthil, A study on compound micromachining using laser and Electric Discharge Machining (EDM), Adv. Mater. Process. Technol. 2 (2016) 258–265, https://doi.org/10.1080/2374068X.2016.1164531.
[134] S. Kim, B.H. Kim, D.K. Chung, H.S. Shin, C.N. Chu, Hybrid micromachining using a nanosecond pulsed laser and micro EDM, J. Micromech. Microeng. 20 (2010), https://doi.org/10.1088/0960-1317/20/1/015037.
[135] A.M.A. Al-Ahmari, M.S. Rasheed, M.K. Mohammed, T. Saleh, A hybrid machining process combining micro-EDM and laser beam machining of nickel–titanium-based shape memory alloy, Mater. Manuf. Process. 31 (2015) 447–455, https://doi.org/10.1080/10426914.2015.1019102.
[136] M.M. Okasha, P.T. Mativenga, L. Li, Microdrilling of Inconel 718 Alloy 133 (2018) 1–8, https://doi.org/10.1115/1.4003334.
[137] A. Schubert, S. Groß, B. Schulz, U. Eckert, Sequential combination of micro-milling and laser structuring for manufacturing of complex micro-fluidic structures, Phys. Procedia 12 (2011) 221–229, https://doi.org/10.1016/j.phpro.2011.03.127.
[138] S. Gross, U. Eckert, J. Edelmann, New sequential manufacturing process for micro and finishing machining, Procedia CIRP 46 (2016) 559–562, https://doi.org/10.1016/J.PROCIR.2016.04.028.
[139] U.M. Attia, S. Marson, J.R. Alcock, Micro-injection moulding of polymer microfluidic devices, Microfluid Nanofluidics 7 (2009) 1–28, https://doi.org/10.1007/s10404-009-0421-x.
[140] Hybrid Machining Processes Perspectives on Machining and Finishing Kapil Gupta Neelesh K. Jain R. F. Laubscher Springer Briefs in Applied Sciences and Technology.
[141] Y.B. Bang, K.M. Lee, S. Oh, 5-Axis micro milling machine for machining micro parts, Int. J. Adv. Manuf. Technol. 25 (2005) 888–894, https://doi.org/10.1007/s00170-003-1950-1.
[142] D. Huo, K. Cheng, F. Wardle, Design of a five-axis ultra-precision micro-milling machine-UltraMill. Part 1: Holistic design approach, design considerations and specifications, Int. J. Adv. Manuf. Technol. 47 (2010) 867–877, https://doi.org/10.1007/s00170-009-2128-2.
[143] X. Luo, K. Cheng, D. Webb, F. Wardle, Design of ultraprecision machine tools with applications to manufacture of miniature and micro components, J. Mater. Process. Technol. 167 (2005) 515–528, https://doi.org/10.1016/J.JMATPROTEC.2005.05.050.
[144] F. Iqbal, S. Jha, Closed loop ball end magnetorheological finishing using in-situ roughness metrology, Exp. Tech. 42 (2018) 659–669, https://doi.org/10.1007/s40799-018-0284-8.
[145] D. Wu, H. Wang, K. Zhang, B. Zhao, X. Lin, Research on adaptive CNC machining arithmetic and process for near-net-shaped jet engine blade, J. Intell. Manuf. 31 (2019) 717–744, https://doi.org/10.1007/s10845-019-01474-z.
[146] F. Iqbal, Z. Alam, D.A. Khan, S. Jha, July. Localized finishing by ball end magnetorheological finishing process using integrated confocal sensor for in-situ surface roughness measurement, in: In *39th International MATADOR Conference on Advanced Manufacturing*, 2017, pp. 5–7.
[147] F. Iqbal, S. Jha, Experimental investigations into transient roughness reduction in ball-end magneto-rheological finishing process, Mater. Manuf. Process. 34 (2019) 224–231, https://doi.org/10.1080/10426914.2018.1512131.
[148] D.R. Unune, H.S. Mali, Current status and applications of hybrid micromachining processes: A review, Proc. Inst. Mech. Eng. Part B J. Eng. Manuf. 229 (2015) 1681–1693, https://doi.org/10.1177/0954405414546141.
[149] C.R. Dandekar, Y.C. Shin, J. Barnes, Machinability improvement of titanium alloy (Ti–6Al–4V) via LAM and hybrid machining, Int. J. Mach. Tools Manuf. 50 (2010) 174–182, https://doi.org/10.1016/J.IJMACHTOOLS.2009.10.013.
[150] Sumit Bhowmik, Divya Zindani. “Hybrid Micro- Machining Processes”, Springer Nature, 2019.
[151] Jitin Malhotra, Faiz Iqbal, Ashish Kumar Sahu, Sunil Jha, A Cyber-Physical System Architecture for Smart Manufacturing, in: Advances in Forming, Machining and Automation, Springer, Singapore, 2019, pp. 637–647.
[152] S.Z. Chavoshi, X. Luo, Hybrid micromachining processes: A review, Precis. Eng. 41 (2015) 1–23, https://doi.org/10.1016/j.precisioneng.2015.03.001.
[153] M. Kumar, S.N. Melkote, Process capability study of laser assisted micro milling of a hard-to-machine material, J. Manuf. Process. 14 (2012) 41–51, https://doi.org/10.1016/j.jmapro.2011.09.003.
[154] T.L. Perry, D. Werschmoeller, X. Li, F.E. Pfefferkorn, N.A. Duffie, Pulsed laser polishing of micro-milled Ti6Al4V samples, J. Manuf. Process. 11 (2009) 74–81, https://doi.org/10.1016/j.jmapro.2009.10.001.
[155] E.V. Bordatchev, A.M.K. Hafiz, O.R. Tutunea-fatan, Performance of laser polishing in finishing of metallic surfaces (2014) 35–52, https://doi.org/10.1007/s00170-014-5761-3.
[156] H. Xia, G. Zhao, J. Yan, L. Li, N. He, X. Hao, Study on laser-induced oxidation assisted micro milling of Ti6Al4V alloy, Int. J. Adv. Manuf. Technol. 103 (2019) 1579–1591, https://doi.org/10.1007/s00170-019-03648-8.
[157] M. Kadivar, B. Azrhoushang, A. Zahedi, C. Müller, Laser-assisted micro-milling of austenitic stainless steel X5CrNi18-10, J. Manuf. Process. 48 (2019) 174–184, https://doi.org/10.1016/j.jmapro.2019.11.002.
[158] Y. Wang, W. Zhang, Theoretical and experimental study on hybrid laser and shaped tube electrochemical machining (Laser-STEM) process, Int. J. Adv. Manuf. Technol. 112 (2021) 1601–1615, https://doi.org/10.1007/s00170-020-06558-2.
[159] M.A.N. Rashid, T. Saleh, W.I. Noor, M.S.M. Ali, Effect of laser parameters on sequential laser beam micromachining and micro electro-discharge machining, Int. J. Adv. Manuf. Technol. 114 (2021) 709–723, https://doi.org/10.1007/s00170-021-06908-8.
[160] K. You, F. Fang, G. Yan, Y. Zhang, Experimental investigation on laser assisted diamond turning of binderless tungsten carbide by in-process heating, Micromachines 11 (2020) 1–15, https://doi.org/10.3390/mi11121104.
[161] W.S. Woo, C.M. Lee, Laser-assisted milling of turbine blade using five-axis hybrid machine tool with laser module, Int. J. Precis. Eng. Manuf. - Green Technol. 8 (2021) 783–793, https://doi.org/10.1007/s40684-020-00217-3.

[162] V.V. Posa, M. Sundaram, Experimental study of micromachining on borosilicate glass using CO2 laser, J. Manuf. Sci. Eng. 143 (2021) 1–7, https://doi.org/10.1115/1.4048639.
[163] L. Zhu, Z. Yang, B. Xin, S. Wang, G. Meng, J. Ning, P. Xue, Microstructure and mechanical properties of parts formed by ultrasonic vibration-assisted laser cladding of Inconel 718, Surf. Coatings Technol. 410 (2021), 126964, https://doi.org/10.1016/j.surfcoat.2021.126964.
[164] D. Kang, P. Zou, H. Wu, W. Wang, J. Xu, Research on ultrasonic vibration-assisted laser polishing of the 304 stainless steel, J. Manuf. Process. 62 (2021) 403–417, https://doi.org/10.1016/j.jmapro.2020.12.009.
[165] H. Wang, Y. Xu, J. Liu, Q. Hu, X. Wang, N. Ren, W. Zhou, X. Ren, Magnet-assisted laser hole-cutting in magnesium alloys with and without water immersion, J. Manuf. Process. 61 (2021) 539–560, https://doi.org/10.1016/j.jmapro.2020.11.026.
[166] J. Yao, B. Li, L. Wang, Electromagnetic Field-Assisted Laser Process, in: Advanced Laser Process for Surface Enhancement. Advanced Topics in Science and Technology in China, vol 61, Springer, Singapore, 2021, https://doi.org/10.1007/978-981-15-9659-9_3.
[167] N. Ren, K. Xia, H. Yang, F. Gao, S. Song, Water-assisted femtosecond laser drilling of alumina ceramics, Ceram. Int. 47 (2021) 11465–11473, https://doi.org/10.1016/j.ceramint.2020.12.274.
[168] Z. Guo, B. Guo, Q. Zhao, W. Liu, Q. Zheng, Optimization of spray-mist-assisted laser machining of micro-structures on CVD diamond coating surfaces, Ceram. Int. (2021), https://doi.org/10.1016/j.ceramint.2021.04.232.
[169] B. Cheng, Y. Ding, Y. Li, J. Li, J. Xu, Q. Li, L. Yang, Coaxial helical gas assisted laser water jet machining of SiC/SiC ceramic matrix composites, J. Mater. Process. Technol. 293 (2021), 117067, https://doi.org/10.1016/j.jmatprotec.2021.117067.
[170] S. Ravi-Kumar, B. Lies, X. Zhang, H. Lyu, H. Qin, Laser ablation of polymers: a review, Polym. Int. 68 (2019) 1391–1401, https://doi.org/10.1002/pi.5834.
[171] Y. Zhang, B. Xie, Investigation on hole diameter non-uniformity of hole arrays by ultrasonic vibration-assisted EDM, Int. J. Adv. Manuf. Technol. 112 (2021) 3083–3091, https://doi.org/10.1007/s00170-021-06597-3.
[172] G. Zhao, H. Xia, Y. Zhang, L. Li, N. He, H.N. Hansen, Laser-induced oxidation assisted micro milling of high aspect ratio microgroove on WC-Co cemented carbide, Chinese J. Aeronaut. 34 (2021) 465–475, https://doi.org/10.1016/j.cja.2020.08.011.